CURJ

ArtCenter College of Design

One of the world's preeminent art and design colleges, ArtCenter College of Design is renowned for its culture of innovation, rigorous transdisciplinary curriculum, superb professional faculty and extensive relationships with industry. For 80 years, Art Center has prepared an influential group of artists and designers to become leaders both in their chosen fields and the world at large.
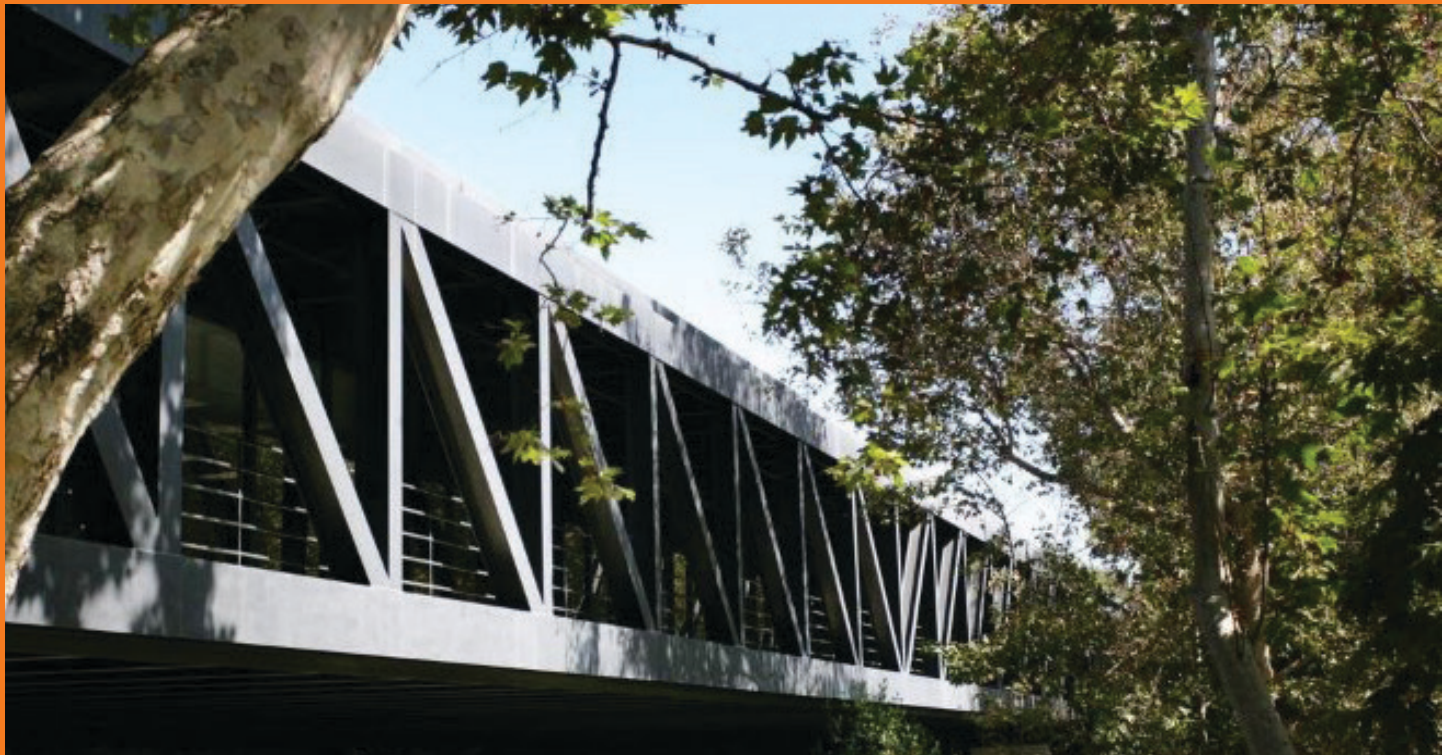
UNDERGRADUATE PROGRAMS

Advertising
Entertainment Design
Environmental Design
Film
Fine Art
Graphic Design
Illustration
Interaction Design
Photography and Imaging
Product Design
Transportation Design

GRADUATE PROGRAMS

Art
Environmental Design
Film
Graphic Design
Industrial Design
Media Design Practices
Transportation Systems and Design

CURJ is a collaborative effort by students at ArtCenter College of Design and the California Institute of Technology.

ArtCenter

Suchita Nety
Editor In Chief

Nils Lindstrom
Art Director

Deb Shieh
Graphic Designer

Joann Shin
Graphic Designer

Ariella Vaystukh
Graphic Designer

Shannon Wang
Content Editor

Minh Nhat Le
Content Editor

Grace Lee
Content Editor

Juliane Preimesberger
Content Editor

Meera Krishnamoorthy
Content Editor

Grace Xiong
Content Editor

Sohpie Ding
Content Editor

Sherry Wang
Content Editor

Staff Collaborations

Nils Lindstrom
ArtCenter College of Design

Candace Rypisi
Caltech Student-Faculty Programs

Susanne Hall
Caltech Hixon Writing Center

This summer marks the beginning of yet another period of intense undergraduate research at Caltech and JPL. Every year, hundreds of students from around the country and the globe are drawn to Pasadena for ten weeks of research under the leadership of talented faculty mentors. Through the guidance of these dedicated mentors, as well as the tireless efforts of Caltech's Student Faculty Programs office, these students have been able to take their first steps of what will become a long journey of scientific curiosity and discovery.

This issue of the Caltech Undergraduate Research Journal highlights the exceptional research of five young scholars: Natalia Brody, Brian Deng, Andre Liu, Joy Westland, and Aaron Young. With topics ranging from developing virtual reality platforms to perform neuroscience experiments to uncovering molecular mechanisms of stroke disorders to simulating quantum computing design parameters, these five articles exemplify the great diversity of work currently being performed by undergraduate students.
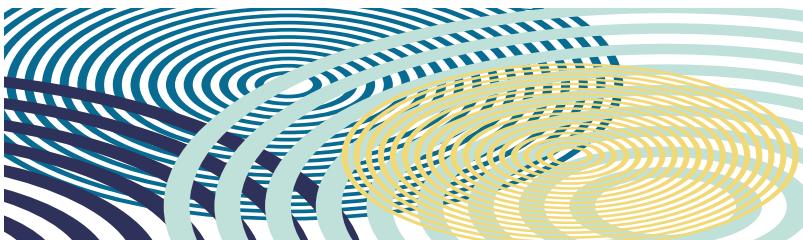
In this issue, CURJ is pleased to feature interviews with two faculty members, Professor Julia Greer and Professor Yisong Yue. We hope you enjoy reading Professor Greer's reflections on being a pioneer in the field of nanoscale materials science and Professor Yue's perspective on machine learning as a growing phenomenon in both industry and academia. Their accomplishments, enthusiasm, and dedication to mentorship serve as an inspiration to all students at Caltech.

We encourage you to visit our website at curj.caltech.edu, where you can find past CURJ issues and more information about the journal. We welcome your comments and feedback. Thank you for picking up this latest issue!

Best regards,

SNety
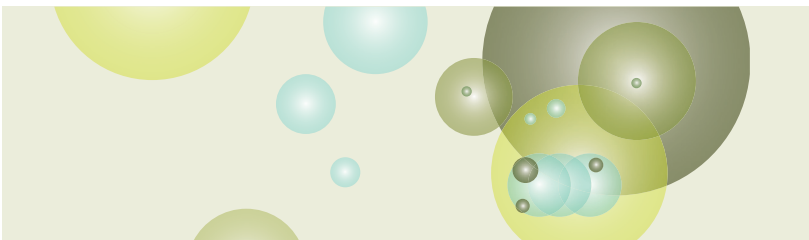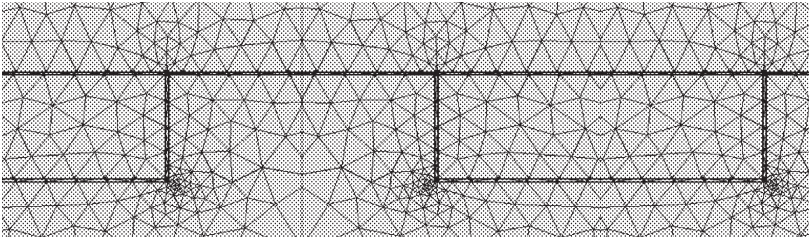
PROFESSOR JULIA GREER received her under-graduate degree in Chemical Engineering from MIT. She simultaneously worked in the Components Research Department of Intel and pursued an M.S. in Materials Sciences at Stanford University. Subsequently, after working at Intel's Mask Operations Department for two years, Julia received a Ph.D. in Materials Science and Engineering from Stanford University, studying size effects in plasticity of metals at the nano-scale with Professor William D. Nix. Prior to starting her appointment as a faculty member at Caltech in June 2007, Greer was a postdoctoral fellow at Palo Alto Research Center. To broaden her expertise, she has worked on investigating the behavior of organic semiconductors—thin film transistors (OTFTs)—as well as nano ink-derived metals for jet-printing in flexible electronics with Dr. Robert A. Street.

Throughout her scientific career, Greer has also been pursuing her "secondary career" as a concert pianist, having studied at the Moscow's Gnessin School of Music, the Eastman School of Music, the San Francisco Conservatory of Music, and at Stanford University. She has performed numerous solo recitals, chamber music concerts, most recently in Lagerstrom Series at Caltech and with the Redwood Symphony.

interview: JULIA GREER

I magine a sheet of paper that is untearable, unbreakable, extremely lightweight, and energy-absorbing. The applications range from armor protection, to extremely lightweight batteries that have a high capacity to store a lot of power, to tiny biomedical devices that can injected as sensors.

What does your lab work on?

We look at materials at the nanoscale, one-hundred-thousandth of the diameter of your hair. Then, we study materials that we are familiar with, and we reduce their dimensions to these very, very small scales. We, and many others, discovered that materials change their properties when you get to these nanometer length scales. Once we discover an interesting property, we then try to use these lucrative properties in larger materials by introducing the concept of architecture into material design. You can envision it by taking a narrow nano-ribbon, whose thickness might be on the order of ten-billionth of a meter, and then wrapping that ribbon conformally around a type of three-dimensional architecture. Very often we use the architecture of periodic lattices; basically imagine a geometrical, three dimensional unit cell, tessellate that unit cell in space, and wrap that nano-ribbon all around it. You end up with these interwoven three-dimensional networks of hollow tubes. When such a material sits on your hand, it looks like a cloud because it's so open: over 99 percent air and very lightweight. Our materials are relatively resilient; we can find better properties in the nano-sized materials, and then through the nano-ribbon approach, we get larger dimensions, but the properties are retained from the nanoscale. Once we have fabricated these nanolattices, we can use them in many different applications, from energy storage in batteries, to implantable biomedical devices, to chemically functionalized sensors or drug attractors in medication.

What are some of the challenges that you face when you are trying to synthesize structures that are incredibly tiny?

It's hard to make materials in the nanoscale. If you think about it, it is relatively easy to make a chunk of copper or a chunk of

We look at materials at the nanoscale, one-hundred-thousandth of the diameter of your hair. We, and many others, discovered that materials change their properties when you get to these nanometer length scales.

gold, but how do you make it very, very thin? There are multiple deposition methods for thin films, but all of these technologies have generally been developed for flat surfaces, like on silicon substrates for microprocessors. Our structures are three-dimensional, with a lot of open spaces; so uniformly depositing something that is very, very thin is quite challenging. Another challenge is that some of these depositional processes require high temperatures; but our nanolattices are initially made out of a polymer, and polymers burn! So we have to use all sorts of tricks, like coating them with a sacrificial layer.

Another major challenge is studying the kinds of microstructures we get. We have something that is bigger than atoms and electrons, which is what physics or chemistry studies, but smaller than continuum, which is what mechanics and mechanical engineering studies. When you use these depositional processes at the nanoscale, you start approaching these thicknesses of tens of nanometers, which actually approaches the size of the microstructure, or the characteristic length scale at which we work. Because of that, it is challenging to get the microstructure that you want, as well as assess it. And then, once you assess it, how can you improve it? The interplay between the length scales is challenging.

What inspired you to go into nanomaterial science?

My undergraduate degree is actually in chemical engineering, and I mostly worked with liquids and gases; I didn't really know solids very well. After I graduated from MIT, I got an internship at Intel, and people at Intel really cared about metals, which they used in microprocessors. So I got involved in studying microprocessors, and thought, hey, material science is actually pretty cool! I went to Stanford for my PhD, and one of the projects was about making nanopillars out of metals and seeing how they mechanically behave. I really liked that advisor, so I started working on the project. I made nanopillars out of gold, and discovered that they were actually

strong, even though gold is typically malleable. Was this a real discovery, or some kind of fluke? And so we did a lot more experiments. After this discovery, we sort of started this field of nanoscale plasticity. I always wondered in the back of my mind whether we could use these nanopillars as nano-LEGO blocks for construction. That's how the idea of architecture was born; the Eiffel Tower looks like several trusses put together. The idea is that we could use these nanopillars to create a small-scale version of that, and because each nanopillar is so strong, an entire structure of nanopillars must also be strong.

What do you enjoy about being a researcher?

The sense of discovery. When you do research, it's exhilarating, because no matter what you do, you will discover something. Sometimes you discover things that completely blow your mind, because you wouldn't have predicted them this way. You know, we all do smart research—we don't just say, "Oh, I wonder what this is going to be like." We think, "No one has ever done this before, and it seems like it ought to happen." Then we formulate a hypothesis and test it. Sometimes the hypothesis holds true, which is very satisfying. Other times, it really doesn't, and you have to think about what that means. In research, unlike in homework problems, there are no answers at the end of the book, so you are responsible not only for gathering the data but asking whether the results are real, and not some kind of experimental artifact. I'm an experimentalist, so I sometimes have to rely on theories developed by others. The kind of experiments we do are one-of-a-kind, and that's really, really exciting.

What is your philosophy on mentorship?

The best part of being a professor, as opposed to just a researcher, is my students. I have a large group of fantastic students, and I know each one of them individually. I talk with them, I connect with them, and it's really rewarding work. I

think it is important to give everyone enough independence, so that they can go and try out ideas on their own. Being a mentor is a little bit like parenting; you are watching your children grow up: they all come in as bright students, and they come out being mature scientists. The opportunity that I have to facilitate this transformation is the best part about mentoring.

What do you envision the applications of nanoscale structures will be in the future? Where do you think the field is headed?

The major obstacle right now for these kinds of nanolattices is scalability. Right now, nobody has a manufacturing process that can print sheets of them, which is the most aggressive pursuit for us right now. Imagine a sheet of paper that is untearable, unbreakable, extremely lightweight, and energy-absorbing. The applications range from armor protection, to extremely lightweight batteries that have a high capacity to store a lot of power, to tiny biomedical devices that can be injected as sensors.

What advice do you have for undergraduates planning to go into research?

Number one: you should all go to grad school! When you are in grad school, choose your advisor wisely, because that is the most important decision that you make. For undergrad, what matters the most is what school you go to, but for grad school what matters is which research group you join. It takes about five years to get a PhD, and you are working side by side with your advisor for those five years. The research that you will be doing will probably be interesting and neat no matter what, but choose your advisor very wisely. ◼

Background images by Daniel J. Kim

Being a mentor is a little bit like parenting; you are watching your children grow up: they all come in as bright students, and they come out being mature scientists.

PROFESSOR YISONG YUE is an assistant professor in the Computing and Mathematical Sciences Department at the California Institue of Technology. He was previously a research assistant at Disney Research. Prior to that, he was a postdoctoral researcher in the Machine Learning Department and the iLab at Carnegie Mellon University. He received his Ph.D. from Cornell University and a B.A. from the University of Illinois at Urbana-Champaign.

Professor Yue's research interests lie primarily in the theory and application of statistical machine learning. He is particularly interested in developing novel methods for spatiotemporal reasoning, structured prediction, interactive learning systems, and learning with humans in the loop. In the past, Yue's research has been applied to information retrieval, recommender systems, text classification, learning from rich user interfaces, analyzing implicit human feedback, data-driven animation, behavior analysis, spots analytics, policy learning in robotics, and adaptive routing and allocation problems.

interview: YISONG YUE

Data science is a very hot field nowadays. The digital world that we live in generates a lot of data that a lot of engineers and scientists are interested in investigating.

What does your research focus on?

My research is on machine learning, or artificial intelligence, which broadly speaking is the idea of using data to help develop computer systems that can automatically make intelligent decisions, nowadays in increasingly more complex scenarios. I previously did research on data-driven animation. Rather than have an artist manually animate every aspect of a cartoon character, we worked on developing a data-driven method to automatically do some of that work, so the artist can focus more on creative processes.

How has your time at Disney prior to Caltech shaped your current research?

Before I joined Caltech, I spent one year as a research scientist at Disney Research. My role there was to take the data sets they had collected over the years and use machine learning methods to derive automated approaches that would help them in many tasks. For example, we worked on using machine learning to animate mouth movements of animated characters. My collaborators at Disney hired an actor, and they asked him to speak pre-defined sentences for ten hours. As he was speaking, every small movement of his lips was tracked very carefully. This data was then used to train a machine learning algorithm that would do automated lip syncing. Lip syncing is one of the most manually intensive and boring tasks that animation artists do. In animations like Frozen, Avatar, or Cars, and whenever an actor in the movie speaks, some artist actually has to manually animate the lips of a cartoon character and synchronize the animation with the speech. That is a manually intensive and costly process, and we developed a procedure that does it automatically.

What I enjoyed about working at Disney Research was that this lab was looking at all of these complicated problems, exciting and exotic problems, different from the kinds of problems you get at places like Facebook, for instance. It was really exciting to think about the best ways to develop machine learning approaches to best make use of this data. I've taken a lot of the lessons I learned there to Caltech, because here at Caltech we also have access to wide range of data sets that are exciting to machine learning researchers in a variety of fields: biology, neuroscience, planetary science, astronomy... they all pose challenges that require careful thinking about how they can be systematically resolved.

How did you become interested in the field of data science?

When I was a first year Ph.D. student at Cornell, I took a class in computer vision, which is the field that studies teaching a computer to recognize patterns and objects and images. The part that I found most interesting about the class was the fact that they were using data to train these models. If you wanted to have a computer vision system that was able to tell whether or not there was a cat in the image, you would use a machine learning approach. You show a program a bunch of images with cats and without cats and then use a machine learning algorithm to automatically train and classify images. Through this class, I learned that if you give a flexible system a data set, it will fit the system to the data. I found that the idea of having these flexible systems, where you don't have to hand code everything, very compelling.

Do you have any career advice for Caltech students who may want to go into data science?

Data science is a very hot field nowadays. The digital world that we live in generates a lot of data that a lot of engineers and scientists are interested in investigating. I would say that it's important to be agile. If you just learn the standard stuff that they teach in class, you will be obsolete in five to ten years. It's important to stay very agile, because the nature of how data is being created is changing. We live in a world where data creation is in a feedback loop. Your interactions on Facebook generate data. Walking around with your cellphone active generates data. Your credit card transactions generate data. You sitting in a self driving car in the future will generate data. As you rely more on digital technology in the future, more data will be generated. So we live in a feedback loop where the

We live in a feedback loop where the data generation process is evolving. Much of data science and machine learning relies on really understanding how this data is being generated.

data generation process is evolving. Much of data science and machine learning relies on really understanding how this data is being generated. Otherwise you use the wrong method for the wrong problem, and you get garbage. It is easy to be tricked into analyzing data in the wrong way, and you get a result, and you apply the result to some product or some system, and the outcome is not what you expect. This happens all the time.

How would you vet those cases?

The most universal solution is a method called cross-valida-tion. I take a data set, and I build a model on that data; I take another, separate data set, and I use this model to make predictions on the second data set. If the model was built properly on the first data set, it should be able to make accurate predictions on the second one. If it does not, then you are doing something wrong. The idea of using an out-of-sam-ple data set to validate your data is a very common practice in machine learning, and is something that will remain very powerful for years to come.

What do you like to do in your spare time?

Now that I've become a professor, I have less free time than I used to. I was in choir for 14 years and I did a lot of acting and theater. I like playing sports and hiking. I play a lot of video games. I still do a subset of that, but mostly pick-up basketball at Braun gym.

### What's your favorite Caltech quirk?

I really like the fact that I get to have such interactive relation-ships with undergraduates. It's not something that's available at every university. In fact, I think Caltech is one of the few schools that let you do this. It's in part due to the small size of the student body. When I was an undergrad, I went to a large state school, so the student to faculty ratio was something like 100 to 1. Here at Caltech I have a handful of academic advisees, which is a size where I can have meaningful rela-tionship with all of them. And I've gotten to know about 50 undergraduates well, which isn't something that would have happened at other schools. I think that's really cool. ∎

Development o:
Reality Platf
Study of Huma
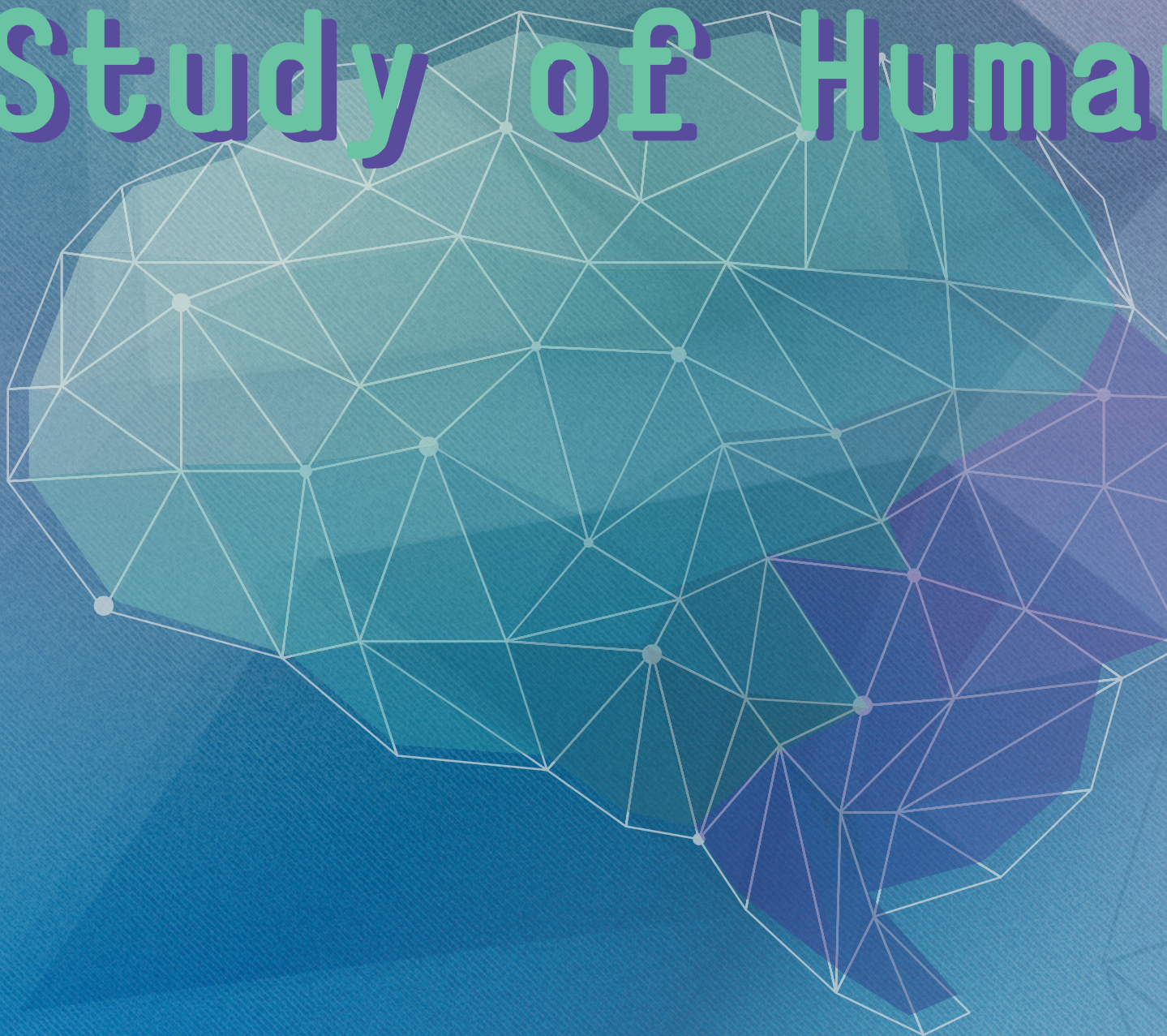
f a Virtual
orm for the
n Behavior

AUTHOR: Natalia Brody, Emory University, Class of 2019
PROJECT PARTNER: Luca Donini, University of Cambridge
MENTORS: Ralph Adolphs, Ph.D. and Juri Minxha, Caltech

ABSTRACT

In the past, neuroscientists have used a single experimental paradigm to study the way we interact with and process the world around us: a subject is shown a stimulus while some form of brain activity (ex. EEG, fMRI, single-units) is recorded. However, the stimulus is typically something simple (i.e., an image, a sound, or a video) and does not reflect the richness of the real world. This project attempts to address this problem by creating a more engaging platform for neuroscience research via virtual reality. Using the game engine Unity, several virtual environments were designed with threat and reward tasks meant to incentivize spatial exploration. Ultimately, virtual reality is shown to be a valid platform for neuroscience research: it elicits realistic responses, gives access to abundant and rich data, and can be applied to niches difficult to study in real-life scenarios (i.e., fear).

INTRODUCTION

Conventional ways of understanding the brain largely depend on 2D stimuli such as pictures and videos. However, brain functions such as emotion and social cognition require richer stimuli and a more trackable user experience in order to be adequately studied. For example, to begin addressing how PTSD affects the brain it would be necessary to 1) elicit a realistic emotional response that is expected to be altered by PTSD and 2) closely monitor the behavioral and psychophysiological responses associated with this response. This example is applicable to more than PTSD—Autism Spectrum Disorders and common disorders such as ADHD, phobias, and anxiety also require rich stimuli and the ability to closely monitor an individual's experience in order to be best studied. Our project proposes that virtual reality is a fitting tool for studying these types of conditions. In addition to the ability to better evaluate human behavior, data collected in virtual reality (VR) could be compiled to create diagnostic models for neurological disorders. These models could be created by comparing the individual's experience of a certain virtual environment with the experience of someone suspected to have a disorder, or comparing the experience of someone known to have a disorder with someone suspected to have it.

The main goal of this project was to create a more engaging and immersive platform for stimuli via virtual reality that could be used as an alternative to the traditional approach. To achieve this goal, a library of virtual environments and 360° videos were created and presented to subjects in order to examine aspects of VR people respond to and to investigate whether certain stimuli (such as visual or auditory cues) affect decision-making in this context. The project was conducted in two parts. The first part of the project was a pilot program in which numerous draft virtual environments were built and used to evaluate various aspects of VR. The second part of the project, "Experimental Study" consisted of a finalized game environment that was presented to subjects in a formal experimental settings.

METHODS

PRELIMINARY GAME DESIGN

Unity game engine is a platform used to develop video games for PC, consoles, mobile devices, and websites. Over the course of this project, Unity was used to build a library of virtual environments that could then be displayed in an Oculus Rift virtual reality headset. To begin, several drafts of potential environments for use in our study were built. Audio, object, and animation packages were purchased from the Unity asset store (an online store through which users can package and distribute their Unity creations to other users) to include in the scenes. Because there are so many possibilities and factors of interest available for manipulation in VR, multiple draft environments were created. Across the various virtual environments, a theme of fear was maintained that would serve as a metric for measuring whether VR was realistic enough and its ability to elicit a strong emotional response (in this case, fear) from a subject. For example, a subject could encounter a frightening monster and, if they had an adverse reaction to this encounter, it could help demonstrate VR as an engaging form of stimuli that evokes reactions parallel to those that would occur in the real world.

The environments created for our library all have similar structure as exploratory spaces that contain both threats and rewards. Threats vary from wolves to zombies and other monsters, while the reward, collectible gold coins, remains the same across environments. This threat and reward system was included in order to incentivize spatial exploration (i.e. wanting to wander the space in order to obtain rewards) and to demonstrate that although virtual, components of virtual reality can influence decision making and the way one explores his environment. Additionally, 360° videos were included in the project library. These videos were sent to the Oculus Rift through Vrideo, an application that distributes immersive videos for use in virtual reality. The purpose of these videos was to give a broader understanding of how subjects interact with and respond to certain aspects of VR.

Pilot Program

After the project library was completed, a pilot program was created so that members of my lab could explore the environments and videos and give feedback. To collect feedback on the library environments, questionnaires were created using Qualtrics. Qualtrics is a tool that creates surveys for research purposes and offers a wide range of features for creating survey questions and analyzing response data. There were a total of three Qualtrics questionnaires: one to review an environment, one to review a video, and one to make comparisons about all of the environments and videos explored. Through the feedback collected, which features of VR are most and least effective were identified. This information was then used to refine current virtual environments and, in the future, can be used as a guide for research-motivated VR game design.

SECONDARY GAME DESIGN

After the pilot program, a more complex virtual environment was created for the second phase of the project, a formal experimental study. Thus, a partnership with White Door Games game developer was started and permission to use their VR video game, Dreadhalls, for the project was obtained. The terms of this partnership allowed for access to and modification to the game's source-code in order to meet the project's needs. Modifications included adding a timer, a coin counter, a map with customized visibility, and variability to maze structure. Unlike the free-roaming and spacious environments built for the first pilot program, Dreadhalls restricted user mobility. The game had a maze-like structure that forced the subject to travel down narrow hallways and make frequent decisions as they traverse from one side to the other. This format allowed for the investigation of decision-making in the presence of threat OR of threats in the environment, and to understand how certain conditioned stimuli (such as a seemingly innocuous sound which becomes predictive of threat) can affect how subjects explore the maze. Overall, this data driven approach aimed to extrapolate trends regarding strategy and decision making in order to further verify that VR engages the user and provides insightful data on behavior.

Experimental Study

A second trial was created, through which Dreadhalls would again be used to further evaluate the suitability of VR as a platform for neuroscience research. Like the pilot program, participants would experience the environment(s) being tested and then provide feedback on a Qualtrics questionnaire. For this pilot program, a new set of questionnaires specific to Dreadhalls were provided. Subjects were recruited by sending emails to the Caltech "houses" (dormitories). Upon arrival, subjects were administered game instructions and game controller instructions. Each subject was given 45 minutes to attempt the game as many times as they wanted. Each participant received a minimum of $10 for participation, but could increase their award based on how many coins they collected (COINS bonus) and whether they reached the maze exit within the game (EXIT bonus). After the participant finished, they completed the questionnaire and received their monetary reward.

COMPUTER-CONTROLLED VARIABLES	PLAYER-CONTROLLED VARIABLES
Choice of map	Position of player (body and head)
Position of monsters	Rotation of player (body and head)
Position of coins	Distribution of monsters (if they follow player)

Participation reward + COINS bonus + EXIT bonus = total monetary reward

EXPERIMENT SETUP

Pilot Program & Experimental Study

Virtual environments were presented on an Oculus Rift that was connected to a PC. This PC ran the VR software while the headset presented the visual stimuli. Audio stimuli were presented through a pair of over-ear headphones. Subjects navigated the virtual environment with an Xbox controller. To avoid risk of physical injury, subjects sat in a swivel chair while experiencing the virtual environments. The chair offered 360° of rotation should the subject desire to turn his body. Questionnaires were presented on a Macintosh computer in the same room.

Experimental Study only

Before participating in the experiment, all subjects filled out a consent form. Game instructions were presented on a Macintosh computer via a PowerPoint presentation. After the experiment, a receipt of the subject's monetary reward was completed.

Virtual reality is shown to be a valid platform for neuroscience research: it elicits realistic responses, gives access to abundant and rich data, and can be applied to niches difficult to study in real-life scenarios (i.e., Fear).

DATA ANALYSIS

The data collected through the questionnaires was related to the user experience and dealt with realism, immersive-ness, task design, and game design. To analyze the collected data, questionnaire responses from the two pilot programs were inputted into Excel and then collected into a number of graphs and trend lines. These graphs provided insight into the user experience at emotional and social levels. The findings these figures provided are significant because they legitimize more complex data (physiological data like eye movement, body position, head orientation) analyzed by my partner—if subjects tended to feel the VR environment was realistic and its task was feasible, it is likely that they responded in VR the same way they would respond in a real life scenario. Verifying that users felt engaged, immersed, that the environment was real, and that the task was feasible supports the project hypothesis that VR will elicit realistic responses and ensures the physiological data is meaningful.
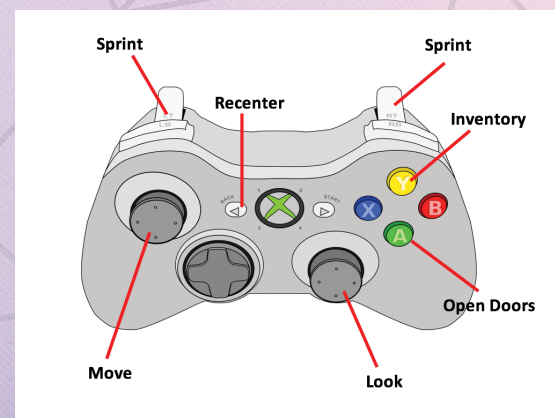
Controller configuration subjects used.

RESULTS

The results of this project indicate that VR is a suitable platform for neuroscience research. Using a simple exploration experiment, users are shown to be much more engaged by this new stimulus presentation method (Figure 3) and that the data that is collected is much more abundant and complex than what is typically collected with on-screen stimulus presentation.

In the experimental study, there were 6 participants. 5 had never experienced VR before and all 6 had never played Dreadhalls before. Immediate observations of the user experience included jumping back in response to startling scares, developing goosebumps, and sweating. Data collected during the experiments verified the usability of the game environment. As subjects continued to play the game, their ability to engage with and learn about the virtual environment improved (Figure 2).

5 out of 6 participants said they felt dizzy or nauseous while in the VR. However, this did not deter subjects from participating—although they had the option to stop at any time, participants attempted the game an average of 4 times. Potential improvements and solutions to nausea induced by VR are addressed in the next section.

Additionally, participants rated evaluative statements about Dreadhalls on a seven-point scale that ranged from completely disagree to completely agree. Ratings collected from these statements positively indicated the user experience was realistic and engaging. The questionnaire results are shown in Figure 1.

	Total Participants	7 (Completely Agree)	6 (Strongly Agree)	5 (Somewhat Agree)	4 (Undecided)	3 (Slightly Disagree)	2 (Somewhat Disagree)	1 (Strongly Disagree)	0 (Completely Disagree)
When exploring the envionrment, I completely avoided the threat.	6	4 67.7%	1 16.7%	1 16.7%	0	0	0	0	0
The objective of the game was clear.	6	5 83.3%	0	1 16.7%	0	0	0	0	0
I felt truly immersed in the game's world.	6	1 16.7%	2 33.3%	1 16.7%	0	1 16.7%	0	0	0

Figure 1
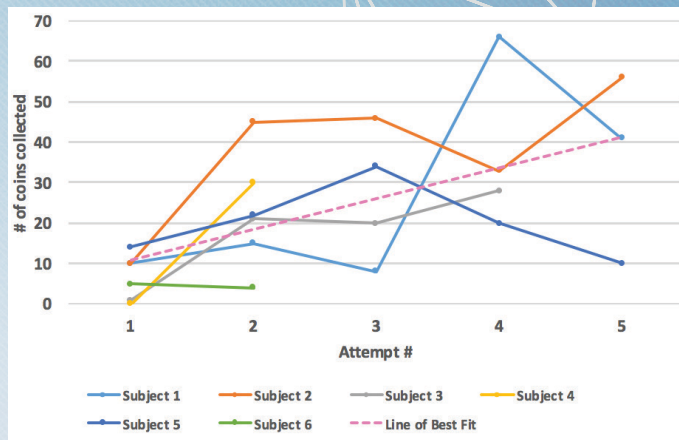Subjects positively rated the overall experience, feasi-bility, and realism of Dreadhalls.

Figure 2
Subjects showed an improvement in strategy; with each attempt, they tended to increase the number of coins they collected.
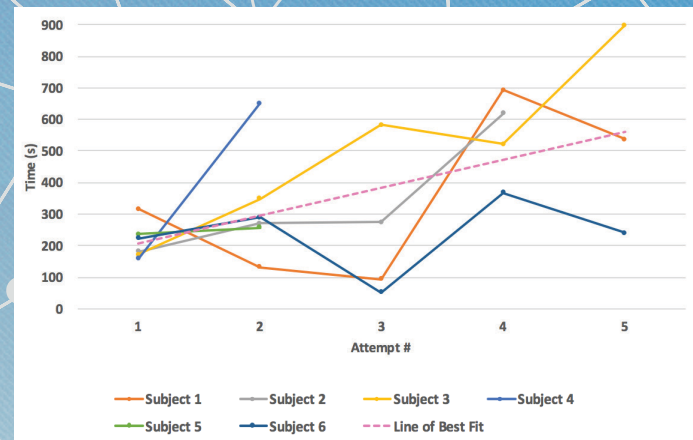
Figure 3
Subjects found the virtual environment to be engaging—although free to stop at any time, there is a positive trend between the amount of time subjects spent in the environment and each attempt. Additionally, all subjects elected to re-enter the environment and attempt its task multiple times.

Figure 4
One example of an exploratory space that was presented to subjects.

IMPLICATIONS & FUTURE DIRECTION

There are numerous avenues for expansion that could be explored, both software- and hardware-based. Environment capabilities could be expanded to include multiple users who engage with each other in virtual reality; this would open up studies to focus on scientific questions regarding social behavior. Additional environments that include richer detail and more similarity to the real world could be built in order to elicit even more realistic responses and more complex behavior. In terms of hardware, subjects could be connected to a biopac while exploring a virtual space. A biopac system monitors psychophysiological data like heart rate, respiratory rate, body temperature, and sweating. An eye tracking device could also be installed on the virtual headset; many VR compatible eye tracker packages are commercially available. Virtual reality could also one day operate in conjunction with a fMRI machine or in sync with electrophysiology so that brain activity could be closely monitored while the user experiences the environment.

It has already been shown that VR is an adequate mode of phobia and anxiety therapy [1], and it is anticipated that our project could set the stage for VR-based diagnostic models. As previously mentioned, the rich and abundant data collected via VR could eventually be compiled into simplistic diagnostic models for disorders relating to how humans perceive and experience the world around them (i.e., anxieties, phobias, etc.); these models would rely on the way that users experience a given virtual environment and then compare it to a neurotypical subject's experience.

In the future, nausea and dizziness induced by VR could be addressed in a number of ways. Possibilities include slowing the ability to quickly change one's field of view with the controller, obtaining new hardware with better resolution, providing pre-experiment training sessions in order to accustom the subject to VR, and limiting time spent in the virtual environment during an experiment. ∎

The rich and abundant
data collected via virtual
reality could eventually
be compiled into simplis-
tic diagnostic models for
disorders relating to
how humans perceive and
experience the world
around them.

FURTHER READING

Opris, D., Pintea, S., García-Palacios, A., Botella, C., Szamosközi, S., & David, D. (2011). Virtual reality exposure therapy in anxiety disorders: a quantitative meta-analysis. Depression and Anxiety,29(2), 85-93. doi:10.1002/da.20910

Brundage, S. B., Brinton, J. M., & Hancock, A. B. (2016). Utility of virtual reality environments to examine physiological reactivity and subjective distress in adults who stutter. Journal of Fluency Disorders,50, 85-95. doi:10.1016/j.jfludis.2016.10.001

Keefe, F. J., Huling, D. A., Coggins, M. J., Keefe, D. F., Rosenthal, Z. M., Herr, N. R., & Hoffman, H. G. (2012). Virtual reality for persistent pain: A new direction for behavioral pain management. Pain,153(11), 2163-2166. doi:10.1016/j.pain.2012.05.030

Hone-Blanchet, A., Wensing, T., & Fecteau, S. (2014). The Use of Virtual Reality in Craving Assessment and Cue-Exposure Therapy in Substance Use Disorders. Frontiers in Human Neuroscience,8. doi:10.3389/fnhum.2014.00844

Finite Element Analysis of the Third Generation Mirror Suspension Systems for Voyager

Joy Westland

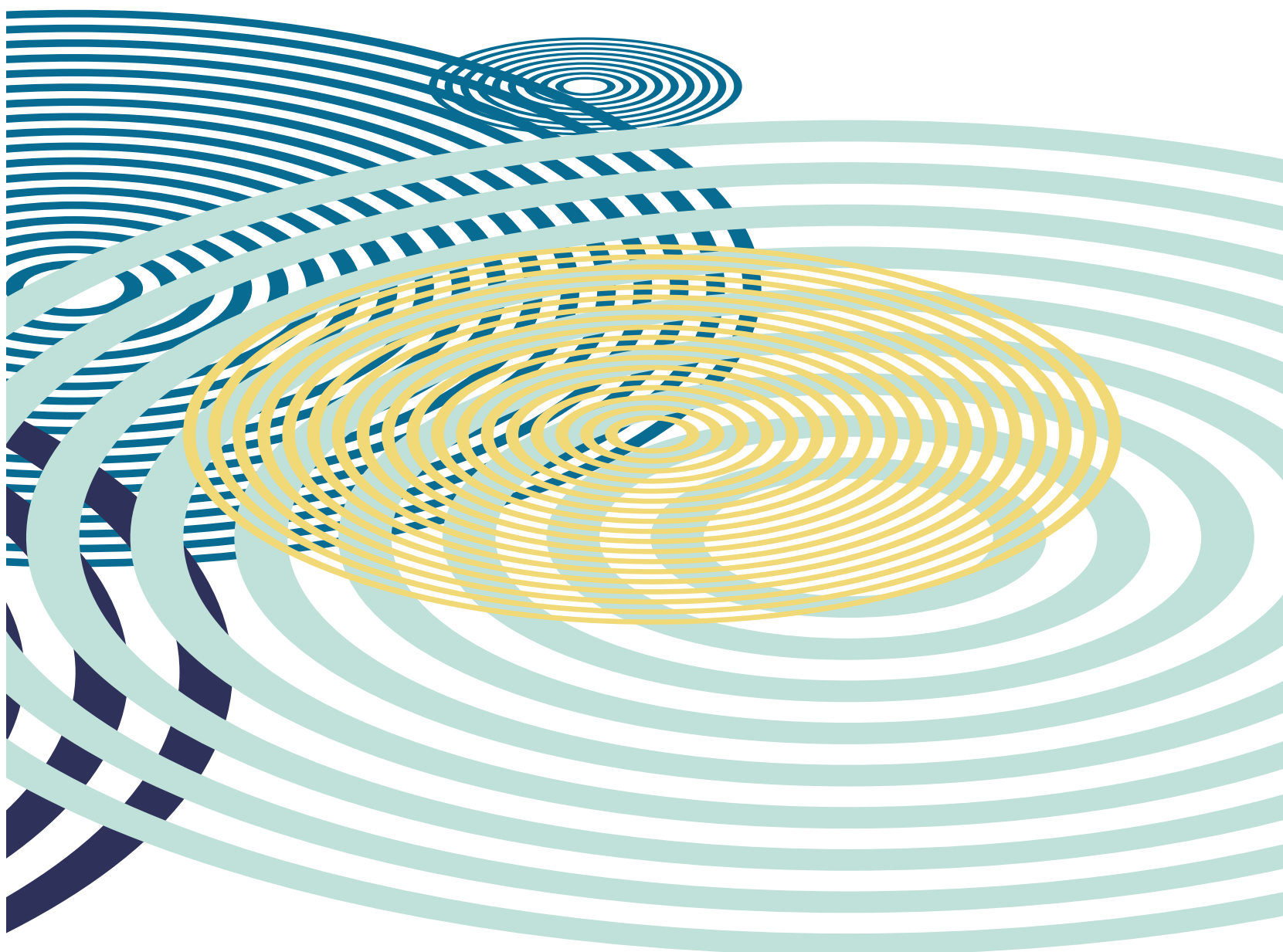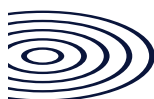Mentors: Alastair Heptonstall and Eric Gustafson
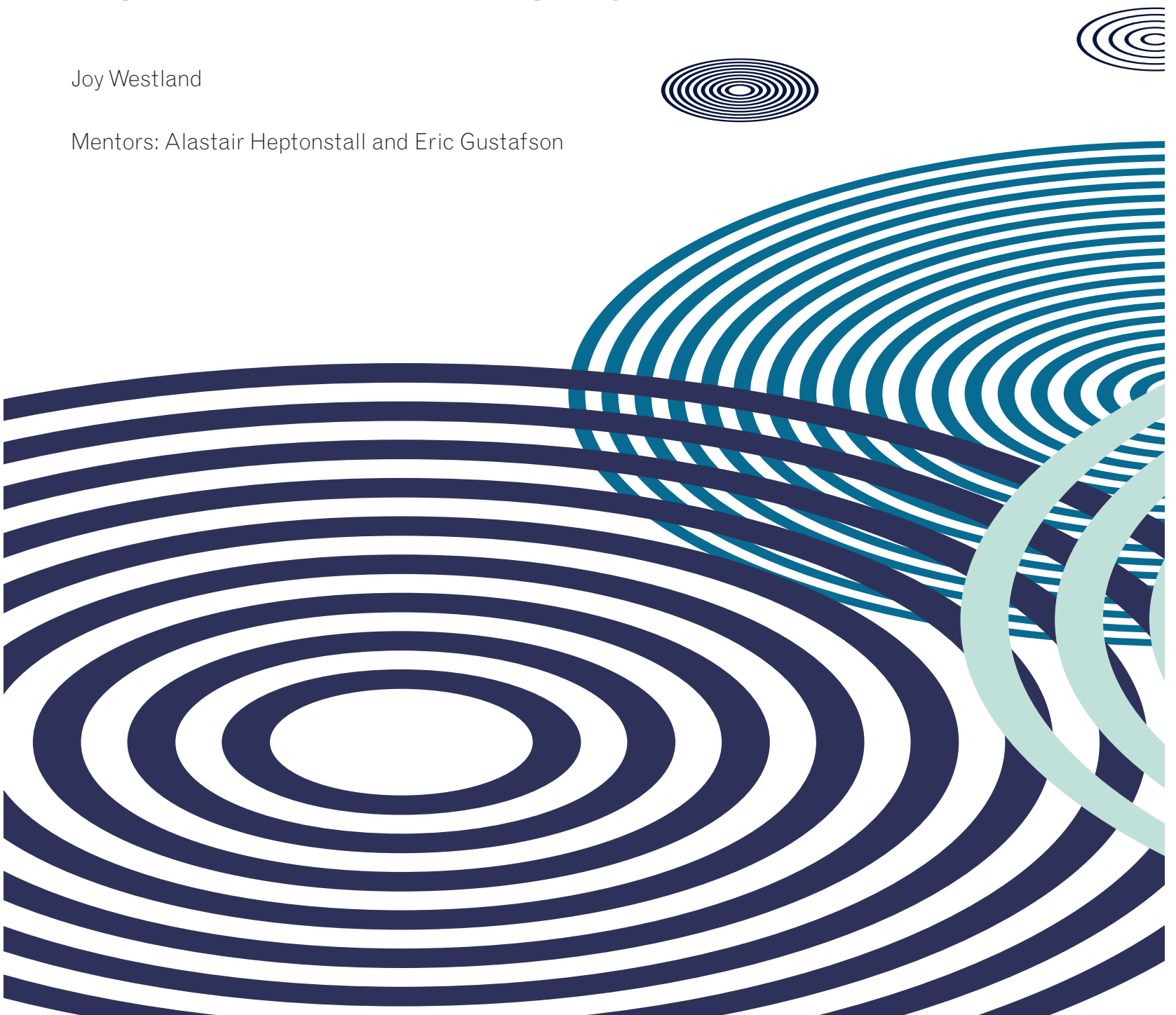
Hometown: Mill Creek, WA
College: University of Washington, Central Washington University
Graduation year: 2018
Major: Dual Degree Physics at Central and Mechanical Engineering at UW with minors in mathematics and industrial engineering technology
Hobbies: Drawing, singing, reading, video games.

Introduction to the Laser Interferometer Gravitational Wave Observatory Advancement

In 1916, Albert Einstein predicted the existence of gravitational waves from the field equations of general relativity. Gravitational waves travel at the speed of light as ripples in the curvature of spacetime (Einstein and Rosen, 1937). Gravitational waves are a strain in space-time caused by accelerating masses. These can be thought of as waves of distorted space being radiated by the source. The U.S. Laser Interferometer Gravitational-Wave Observatory, LIGO, has two facilities located in Hanford, Washington and Livingston, Louisiana. The LIGO detectors are dual recycled Michelson interferometers with Fabry-Perot cavities (Arrain and Mueller, 2008). The facilities were upgraded to improve sensitivity with the aim of achieving a factor of 10 improvement at the most sensitive part of the detection band. On September 14, 2015 a gravitational wave signal was simultaneously detected at both sites (Abbot, 2017), with a second detection following on December 26, 2015.

With the advancing of technology, the main goal for aLIGO is to become more sensitive to detect grav-itational waves from other sources such as neutron-star binary mergers. A few differences between iLIGO and aLIGO are that the input laser power changed from 10 W to 180 W, the mirror mass changed from 10 kg to 40 kg, the power-recycled Fabry-Perot arm cavity Michelson became a dual-recycled Fabry-Perot arm cavity Michelson, the seismic isolation performance improved from 50 Hz to 12 Hz, and the mirror suspensions increased from a single pendulum to a quadruple pendulum (Weinstein, 2012). In Figure 1, the advanced LIGO mirror suspension systems are made of two mirror fused silica test masses. In order to analyze the thermal noise using Finite Element Analysis, we subject the mirrors to various parameters while they are cryogenically-cooled. The test masses are used to reflect LIGO's laser through the interferometer before impacting the photodetector.

The suspension design of initial LIGO had limited sensitivity due to seismic noise and thus needed to be upgraded. Seismic noises come from the natural occurrences such

Three stages of maraging steel blades for vertical isolation

Fused silica fibres

Z

40 kg fused silica test mass
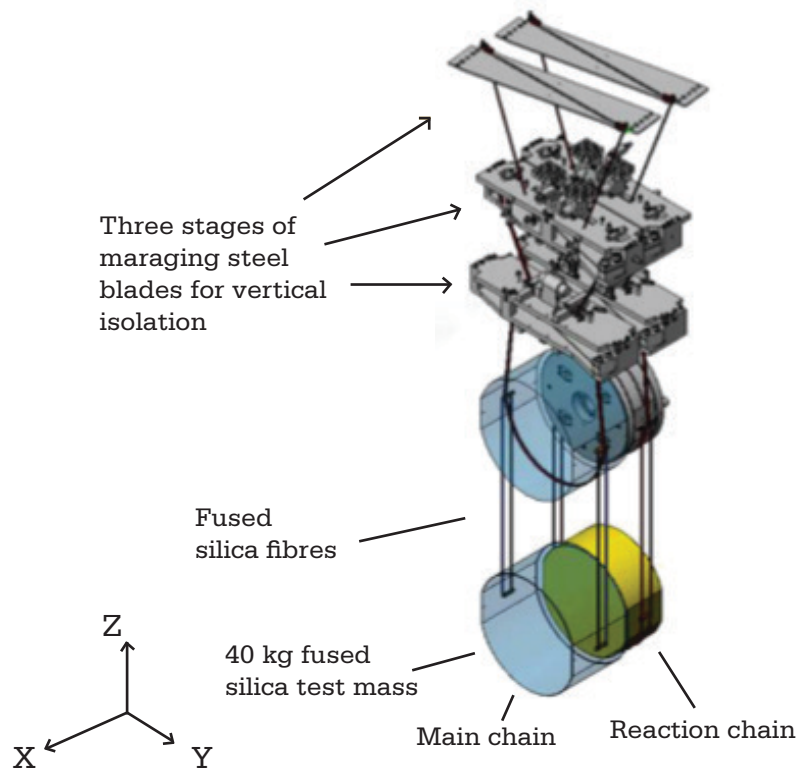
X

Y

Main chain

Reaction chain

Figure 1: Advanced LIGO mirror suspension systems.

as earthquakes and tidal waves to man-made sources such as traffic. Thermal noise results from the thermal energy of atoms and molecules in the mirrors and their suspensions which are at a finite temperature. According to the fluctuation dissipation theorem, off-resonance noise can be reduced by using low dissipation materials in the suspension system, which stores most of this thermal energy close to the resonant modes (Callen and Welton, 1951). There are a number of noise sources that affect the sensitivity of the interferometer gravitational wave detector. The main sources of noise are seismic, gravitational gradient, thermal, and quantum noise.

Physicists hope to increase the amount of advanced gravitational wave networks because a global network of gravitational wave detectors will improve the ability to locate sources in the sky while also increasing the

detection sensitivity. By multiplying the amount of interferometers globally, it will allow the system to enhance the network sky coverage and maximum time coverage. With the increase of interferometers, the detection confidence will increase because there will be an increase of signal detections for a single source. In order to increase the sensitivity, the current research is being done to decrease the different sources of noise.

Motivation for Decreasing Thermal Noise in Advanced LIGO Detectors

The Advanced LIGO mirror suspensions have now been installed (Aston et al., 2012) and research has begun to look at possible future upgrades that would allow thermal noise to be further reduced. The Advanced LIGO suspensions use fused silica for the test masses and fibers. Fused silica helps reduce the amount of off resonance Brownian motion from the atoms and molecules. Brownian motion describes the random motion of particles from the dissipation and fluctuations within the system (Einstein et al., 1926). In order to reduce the thermal noise, one potential process is using cryogenic techniques (Rowan et al., 2005). The focus of this project is to investigate fused silica using Finite Element Analysis (FEA) to analyze their properties as cryogenically-cooled suspension fibers. The main goal of this project is to work towards building a full model suspension system to allow for direct calculation of the mechanical admittance. By using FEA, the project will analyze built models for the gravitational wave detector mirror suspensions, specifically for third generation detectors using a fused-silica hybrid type suspension for the interferometry mirrors.

The Methods Used to Model the Suspension Systems

In this project FEA was performed using the American Computer-aided engineering software known as ANSYS. ANSYS allows a user to use FEA for multiple models using different analyses. The analyses that have been used to become familiar with the program are Modal analysis and Static Structural analysis. The goal is to continue to become familiar with the program in order to begin modeling the actual suspension system. By comparing analytically and computationally, there will be multiple checks on the ANSYS program to ensure the program accounts for the "real world" forces and natural phenomenon correctly. Not only is ANSYS being checked, but also the modeling techniques. This can be seen by the importance of ensuring the models have the correct meshing and mesh density and are built in such a way as to accurately reflect the real physical system. This is important because by accurately describing the mirror suspensions computationally, then experiments will be made with small increments without making a physical suspension system.

Calculating Violin Modes and Frequencies

A simple pendulum model was used to test the accuracy of our ANSYS model when analytically and computationally calculating the violin modes and frequencies. A violin mode is when the fused silica fibers resonate at a certain frequency creating different harmonics, in this case a wave of different nodes. There were two individual pendulum models, one wire had a diameter of 400 microns and the other wire had a diameter of 800 microns. The suspended mass on each wire was 10 kg and the length of each wire was 0.6 m long, shown in Figure 2. These values were chosen because aLIGO fiber suspensions are 400 microns in diameter, suspending 10 kg per wire.

The reason behind starting with a simple pendulum model was to check how ANSYS calculated the violin modes for a uniform wire. The complexity of the full suspension system increases processing power and in order to not waste time, smaller steps have been made to check that ANSYS is taking account of all factors. The actual fibers for the suspension system are tapered at the ends with varying diameters, which causes difficulty in analytically solving the violin modes by hand. By using a uniform fiber and analytically calculating the violin modes, the results can be compared reasonably to ANSYS in order to ensure that ANSYS is accurate. This will increase confidence in the program when using Finite Element Analysis (FEA) for the larger suspension system. The analytical equation for solving the violin frequencies was derived by Willems et al. (2002) which describes:

$$f_n = \frac{n}{2l}\sqrt{\frac{T}{\rho_l}}\left[1 + \frac{2}{l}\sqrt{\frac{EI}{T}} + \frac{EI}{2T}\left(\frac{n\pi}{l}\right)^2\right]$$
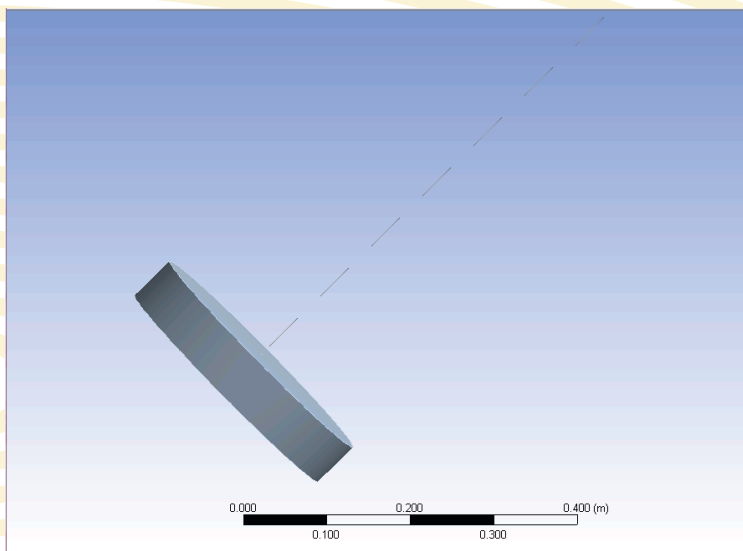

Figure 2: Simple pendulum model where the wire diameter is 400 microns with a length of 0.6 m and an attached mass of 10 kg.

For each different diameter of the wire, MATLAB was used to analytically solve for each violin frequency, shown in Table 1 and Table 2.

Table 1

Diameter: 400 Micrometers

Analytical		Computational	
Mode	Frequenct (Hz)	Mode	Frequency (Hz)
1	497.74	1	495.3
2	995.25	2	990.62
3	1493.4	3	1486
4	1991.3	4	1981.5
5	2489.5	5	2477.2
6	2987.8	6	2973
7	3486.3	7	3469.1
8	3985.1	8	3965.3
9	4484.2	9	4461.9
10	4983.6	10	4958.8

Table 2

Diameter: 800 Micrometers

Analytical		Computational	
Mode	Frequenct (Hz)	Mode	Frequency (Hz)
1	251.3	1	251.09
2	502.9	2	502.49
3	755.1	3	754.48
4	1008.2	4	1007.4
5	1262.6	5	1261.5
6	1518.4	6	1517.1
7	1776	7	1774.4
8	2035.8	8	2033.9
9	2297.9	9	2295.7
10	2562.8	10	2560.1

Table 1 and Table 2: Calculation of the violin modes and frequencies, both analytically (MATLAB) and computationally (ANSYS), of a clamped pendulum for different diameter wires. The wire diameters were 400 microns and 800 microns. The mass attached at the end of both pendulums was 10 kg.

The results from the analytical solution were within 0.5% or below compared to the computational solution.

With this confirmation of the violin modes, then further study will go towards increasing the complexity of the model from a simple pendulum to the bottom stage of the mirror suspension system. The tapered thickness of the actual fibers can be analyzed using ANSYS through FEA. This will then be compared to other experimental ANSYS results in different studies in order to get a sense of using ANSYS towards modeling the full suspension system.

Calculation of Thermal Noise of the Pendulum System from a Gaussian Pressure

Described by Levin, internal thermal noise can be calculated directly, by applying a pressure that mimics the light beam intensity and then calculating the energy dissipated in the mirror and suspension (Levin, 1998). A Gaussian pressure was applied to a face of a test mass with only the ears and a test mass with both the ears and fibers. The strain data was then exported from the test mass, ears, and fibers. The Gaussian pressure as a function of the radius can be shown from Coyne as

$$f(r) = \frac{1}{\pi (r_o)^2} \, e^{-\frac{r^2}{(r_o)^2}}$$

where is 1.56 cm. In Figure 3 the Gaussian pressure is shown in the static structural analysis of ANSYS on the face of a test mass without wires.

The thermal noise can be calculated using Levin's formulation:

$$S_x(f) = \frac{2k_B T}{\pi^2 f^2} \, \frac{W_{\{diss\}}}{F_0^2}$$

The strain energies were extracted from ANSYS in order to find the total loss angle of the system. While Levin's formulation of thermal noise

allows the direct calculation of it, the method to follow Cumming et al., was used instead. This is where ANSYS is used to find the total loss in the system and then use a modal summation technique to calculate the resulting thermal noise. An analytical calculation using MatLab was used to calculate the power spectrum of displacement noise for a single pendulum with four wires. The noise calculation was made by using a modal summation of a pendulum and vertical modes for a 40kg mass made out of fused silica with 60cm length wires. In Table 1 the strain energies are shown for separate sections of the suspension. Figure 4 shows the resulting suspension thermal noise for the pendulum mode of the suspended optic.
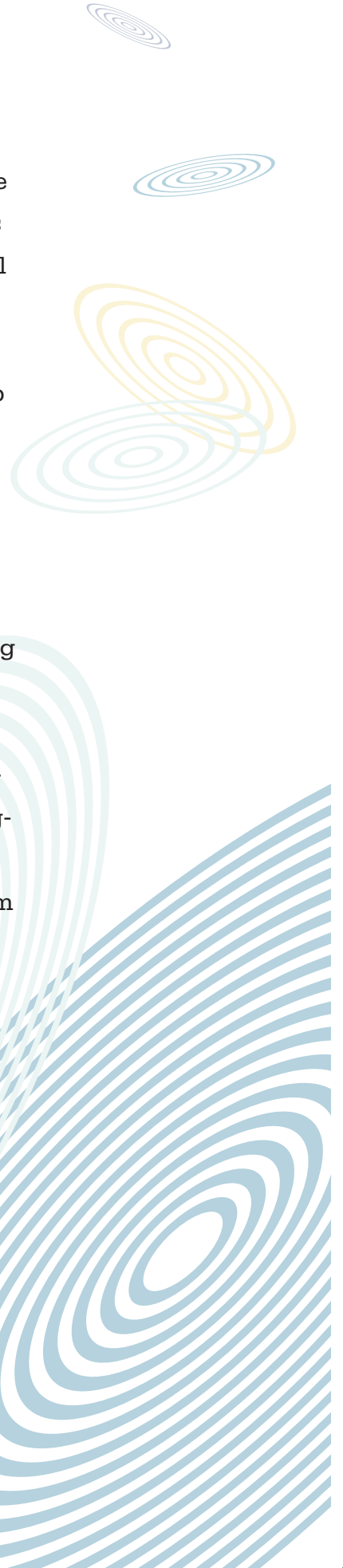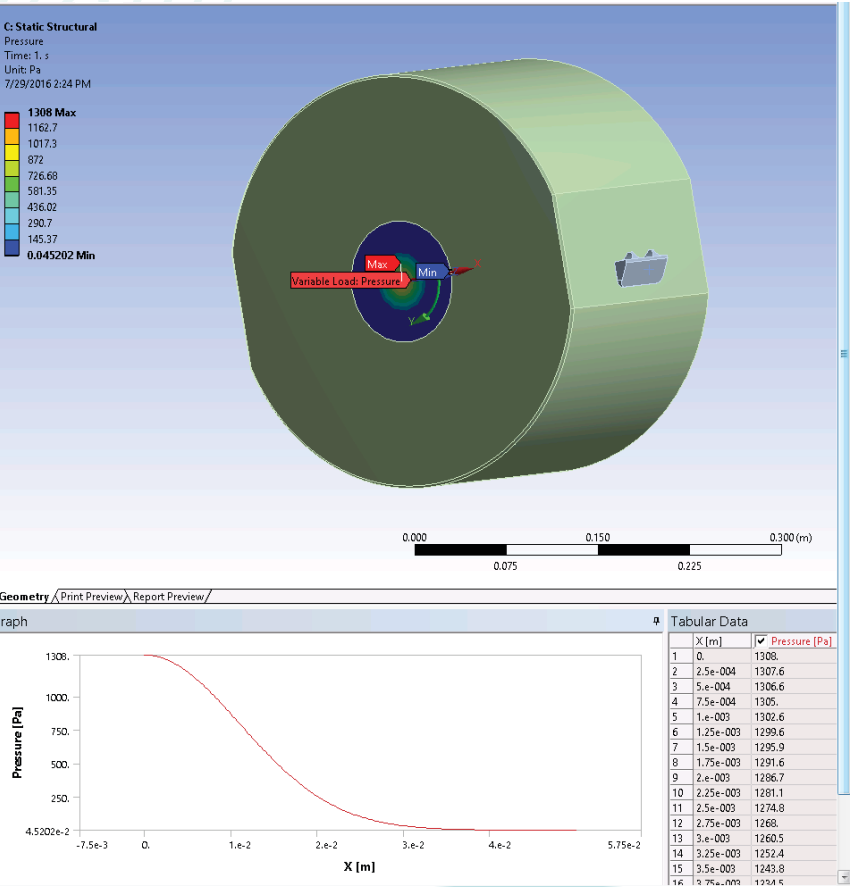
Figure 3: ANSYS model of a Gaussian force applied to the face of an aLIGO optic.

Situation	Strain Energy (J)
Whole Part	1.212
Test Mass Only	1.121E-05
Both Ears Only	1.106E-04
Wires Only	1.212

Table 3: The computational results of the strain energies of the lower stage of the mirror suspension systems using FEA in ANSYS.
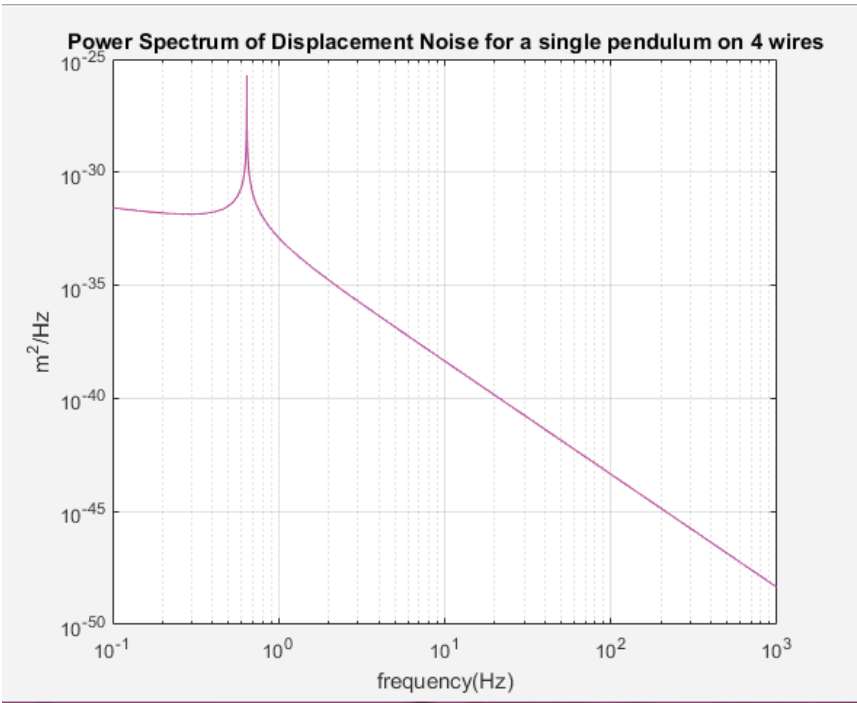

Figure 4: The Gaussian Force once applied to the face of the surface.

These calculations indicate the pendulum mode of the resonance frequency. Fused silica was chosen to be the fibers, test mass, and ears because one of the characteristics of fused silica is a high quality factor (Q). This means that the mechanical loss of fused silica is less. However, when the temperature decreases, the mechanical loss increases. The ongoing investigation into different materials such as silicon and sapphire is due to the decreased Q of fused silica as the temperature decreases. The strain energies can be used to directly calculate the thermal noise of the fibers when calculating

$$W_{\{diss\}} = E_{\{wire\}} \rho_{\{wire\}}$$

Conclusion

In conclusion, the continued effort to understand how to increase the sensitivity in the aLIGO mirror suspension systems will help the overall performance of aLIGO in detecting gravitational waves. The Levin approach allows the direct calculation of the fluctuation dissipation by using the strain energies of the system and the Gaussian force applied to the test mass face. This project was able to calculate the thermal noise and make the first few steps towards computationally calculating

the noise using the Levin approach. The project shows the preliminary results through basic modal summation in order to give approximate measurements of the thermal noise in room temperature fused silica suspension. The final stage of the suspension model was implemented into ANSYS in order to compare the frequencies to the analytical modal summation analysis. Using ANSYS static structural model, strain energies were extracted from the wires. Overall, this project set the ground work for enhancing multiple techniques in using FEA for continual analysis of the suspension system.

Future Goals

The sensitivity curve has yet to reach the full potential of aLIGO and further improvements will be made in increasing the sensitivity. One goal is to calculate the thermal noise in the suspension systems at varying temperatures in order to compare and contrast different material for the test masses. Another goal is to directly apply the Levin technique using FEA in a way that allows us to sweep the frequency of the applied Gaussian force and to directly extract the thermal noise without using a modal summation technique.

The basis of developing the suspension models will ultimately help analyze the performance of cryogenically cooled mirrors. The main goal is to find ways to decrease the thermal noise in the test mass, fibers, and ears. This work will pave the way for future projects in developing and building the full fledged mirror suspension system.
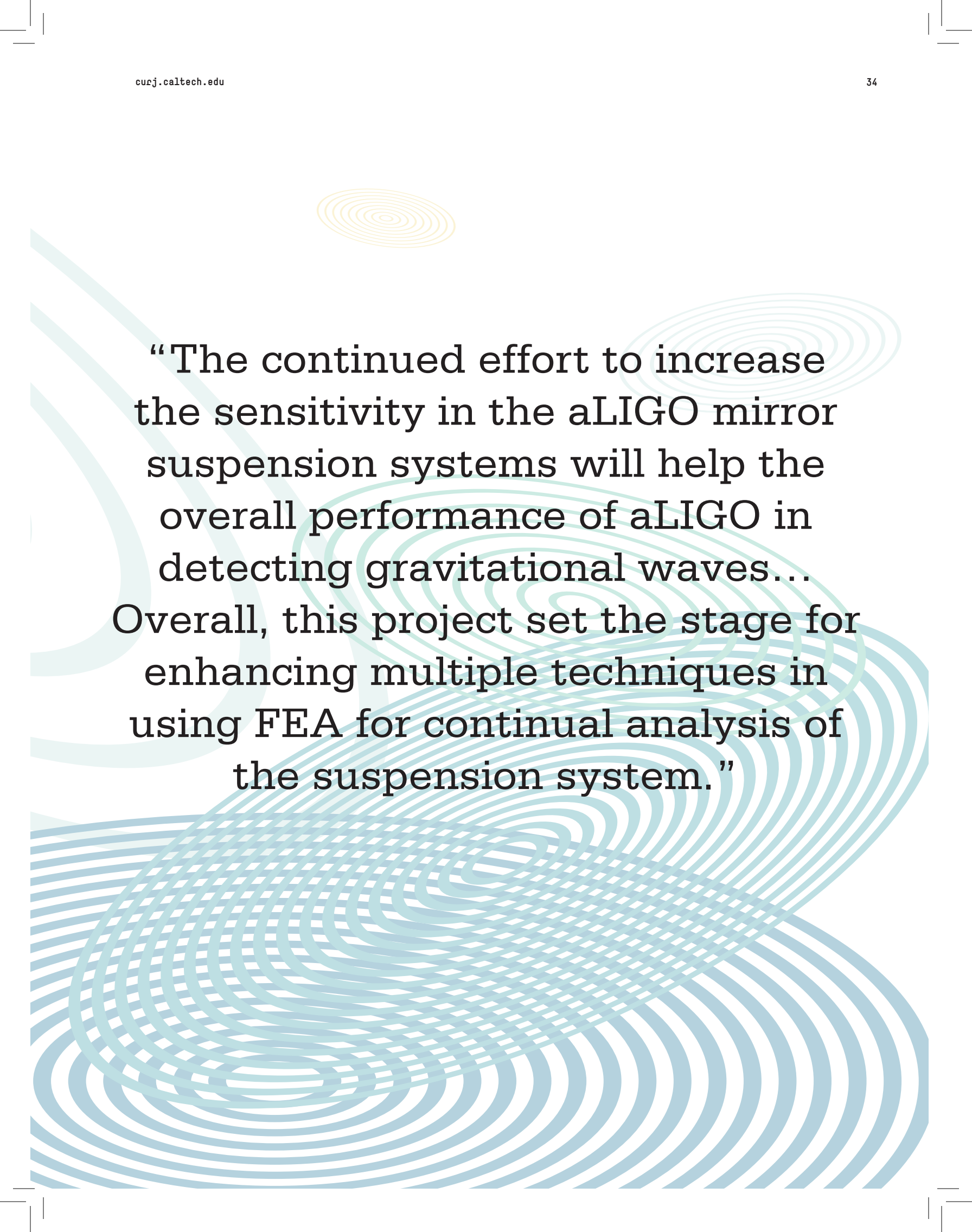
Further Reading

Abbott, B. P. (2017). Observation of Gravitational Waves from a Binary Black Hole Merger. Centennial of General Relativity, 291-311. doi:10.1142/9789814699662_0011

Arain, M.A., and Mueller, G. (2008). Design of the Advanced LIGO recycling cavities. Opt. Express Optics Express, 16(14), 10018. doi:10.1364/oe.16.010018

Aston, S. M., Barton, M. A., Bell, A. S., Beveridge, N., Bland, B., Brummitt, A. J., . . . Wilmut, I. (2012). Update on quadruple suspension design for Advanced LIGO. Class. Quantum Grav. Classical and Quantum Gravity, 29(23), 235004. doi:10.1088/0264-9381/29/23/235004

Rowan, S., Hough, J., \& Crooks, D. (2005). Thermal noise and material issues for gravitational wave detectors. Physics Letters A, 347(1-3), 25-32. doi:10.1016/j.physleta.2005.06.055

"The continued effort to increase the sensitivity in the aLIGO mirror suspension systems will help the overall performance of aLIGO in detecting gravitational waves… Overall, this project set the stage for enhancing multiple techniques in using FEA for continual analysis of the suspension system."

Calcium-Dependent Molecular Mechanisms of CADASIL Disease

Andre Liu
Mentors: Michael Wang and Marianne Bronner

A Quick Overview

Cerebral autosomal dominant arteriopathy with subcortical infarcts and leukoencephalopathy (CADASIL) is the most common inherited cause of stroke. Mutations to the NOTCH3 gene, which controls intracellular signaling pathways, have been linked to CADASIL. However, it is not known how these mutations lead to the onset of the disease. Our lab has found in previous studies that pathological activity of mutant NOTCH3 protein may be due to the reduction of multiple cysteine residues as well as the associated disulfide bonds on this protein. We hypothesized that an N-terminal fragment (NTF) of NOTCH3 catalyzes the formation of multiply-reduced cysteine NOTCH3, which in turn facilitates NTF cleavage from NOTCH3 in a positive-feedback loop.

To investigate potential ways of inhibiting this pathological feedback loop, we aimed to identify factors which control the reaction rate between NOTCH3 and NTF. We found that sequestering calcium ions by supplementing a mixture of NOTCH3 and NTF with EGTA in vitro caused increased NOTCH3 reduction. On the other hand, direct addition of calcium ions by supplementation of $CaCl_2$ to a reaction mixture of NOTCH3 and NTF resulted in decreased NOTCH3 reduction. This suggests that calcium plays a role in slowing or inhibiting pathological NTF-induced NOTCH3 reduction. Thus, cellular calcium levels may be a potential target for future CADASIL treatments.

CADASIL and Its Cause

Cerebral small vessel disease refers to a group of physiological disorders which affect the structure and function of small blood vessels in the brain. These disorders account for a significant percentage of strokes worldwide. Cerebral autosomal dominant arteriopathy with subcortical infarcts and leukoencephalopathy (CADASIL) is an inherited cause of cerebral small vessel disease. CADASIL symptoms typically become evident in middle-aged adults, and include migraine with aura, ischemic stroke, dementia, and abnormalities in the distribution of white-matter in the brain.

CADASIL has been linked to an accumulation of several proteins in small arteries of the brain. One such protein is NOTCH3, a key mediator of intracellular signaling pathways which is present in vascular smooth muscle cells of the cerebral cortex. A gain-of-function mutation in the NOTCH3 protein has been suggested to be the root cause of CADASIL. Nevertheless, it is not clear how this gain of function can lead to a build-up of NOTCH3 in CADASIL patients. A form of NOTCH3 in which multiple disulfide bonds on the protein are reduced ("multiply-reduced cysteine NOTCH3") exhibits characteristics of the mutant NOTCH3 pro-

tein known to cause CADASIL. This reduced form of NOTCH3 contains an N-terminal fragment (NTF) which can be cleaved from the protein. After cleavage, this fragment is then free to reduce disulfide bonds on wild-type NOTCH3, thus increasing the amount of reduced NOTCH3 in a positive feedback loop.

Since the reaction between NTF and NOTCH3 produces the pathological form of NOTCH3, inhibiting this reaction may slow the progression of CADASIL. In this study, we investigate calcium ions as a possible mediator of the NTF-NOTCH3 reaction. We find that calcium ions decrease the NTF-mediated reduction of NOTCH3, while EGTA, which sequesters calcium, increases this reduction. Together, these results suggest that calcium ions inhibit the reaction between NTF and NOTCH3. Thus, regulating calcium levels in cerebral small vessels may be a useful strategy in the treatment of CADASIL.

"Our study introduces calcium as a potential target for novel therapeutic treatments of CADASIL."

The Effect of Calcium on NOTCH3 Reduction

Calcium Supplementation Decreases NTF-Mediated NOTCH3 Reduction:

We first investigated the rate of NOTCH3 reduction in the presence of the chelating agent EGTA, which binds to and removes calcium ions from solution. NTF and NOTCH3-Fc solutions were combined in vitro and incubated for one hour with EGTA. To quantify the amount of reduced NOTCH3, we analyzed samples using fluorescent labeling and immunoprecipitation. We found that adding EGTA to the mixture of NTF and NOTCH3-Fc increases the amount of reduced NOTCH3 (Figure 1). In contrast, control groups where NTF was not added showed little NOTCH3 reduction both before and after EGTA treatment. This suggests that EGTA facilitates the NTF-induced reduction of NOTCH3, possibly by removing Ca2+ from the solution.

	1	2	3	4	5	6	7	8	9	10	11	12
NOTCH3-Fc:	+	+	+	+	+	+	+	+	+	+	+	+
EGTA:	-	-	+	+	+	+	+	+	+	+	+	+
NTF:	-	+	-	+	-	+	-	+	-	+	-	+
$CaCl_2$ (mM):	-	-	-	-	1.8	1.8	3.6	3.6	7.2	7.2	14.4	14.4
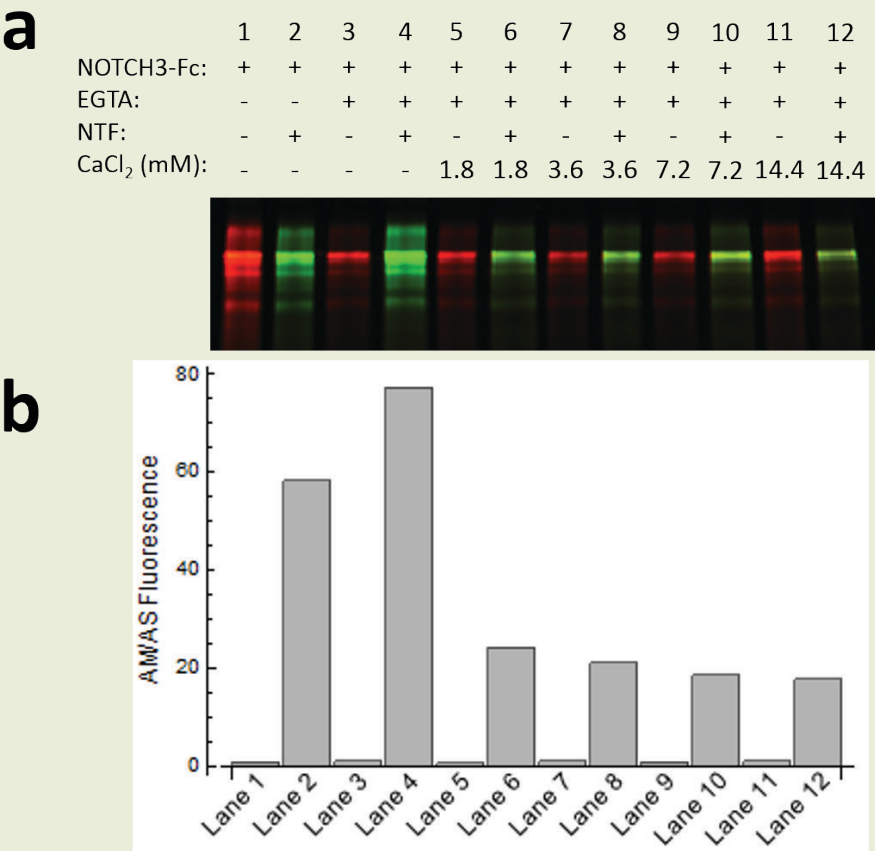
Figure 1 - Effect of EGTA on Reduction of NOTCH3 by NTF

a. Image of PAGE performed on triplicate samples of NTF and/or NOTCH3-Fc incubated with or without EGTA. Fluourescent labels Alexa 700-succinimide (red) and Alexa 800-maleimide (green) were used to label total protein and reduced NOTCH3-Fc, respectively. Repeated 5 times to confirm results.

b. Grpahical representation of relative amount of reduced NOTCH3-Fc to total NOTCH3-Fc present in samples. Data expressed in ratio of Alexa 800-maleimide (AM) fluorescence to Alexa 700-succinimide (AS) fluorescence normalized to background fluorescence. Error bars denote standard deviation of triplicate groups.

Calcium Supplementation Decreases NTF-Mediated NOTCH3 Reduction:

We then investigated whether direct addition of calcium ions could reverse the effect of EGTA. After treatment with EGTA as previously described, samples were incubated with CaCl2 of different concentrations ranging from 1.8 mM to 14.4 mM. Using this method, we found that increasing the CaCl2 concentration decreases the amount of reduced NOTCH3 (Figure 2). Control groups where NTF was not added showed little NOTCH3 reduction regardless of CaCl2 concentration. These results are consistent with the EGTA experiment since both experiments suggest a negative correlation between Ca2+ levels and NTF-mediated NOTCH3 reduction.

a

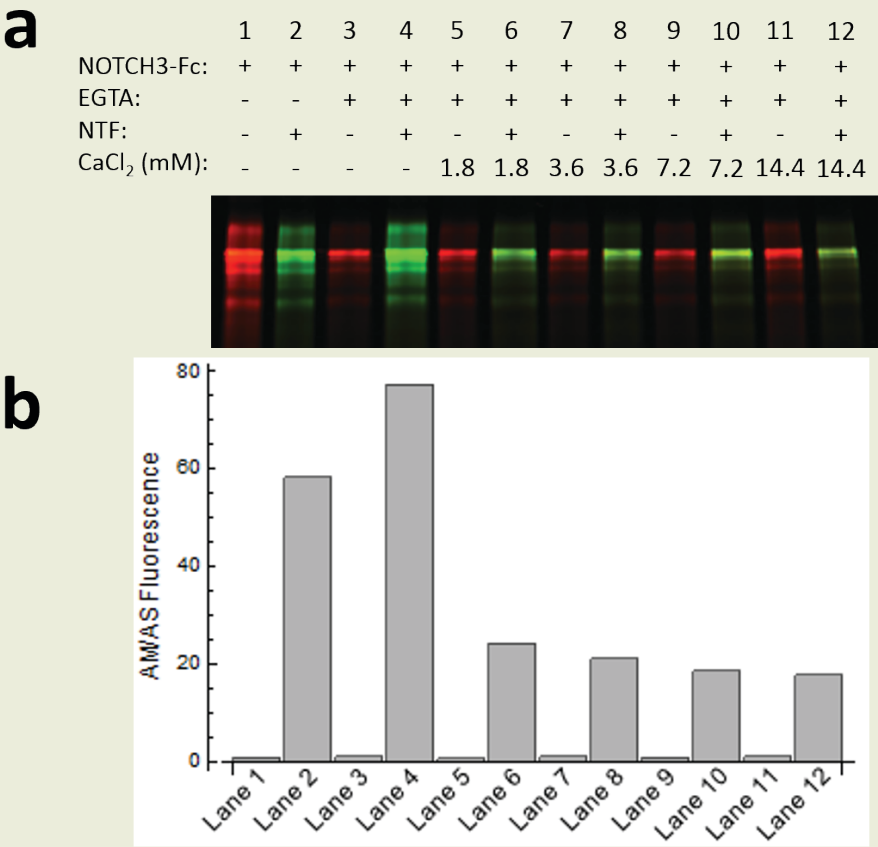|	1	2	3	4	5	6	7	8	9	10	11	12
NOTCH3-Fc:	+	+	+	+	+	+	+	+	+	+	+	+
EGTA:	-	-	+	+	+	+	+	+	+	+	+	+
NTF:	-	+	-	+	-	+	-	+	-	+	-	+
CaCl$_2$ (mM):	-	-	-	-	1.8	1.8	3.6	3.6	7.2	7.2	14.4	14.4

b

Figure 2 - Calcium Supplementation to NOTCH3 and NTF

a. Image of PAGE performed on samples of NTF and/or NOTCH3-Fc incubated with EGTA and varying concentrations of CaCl2. Fluorescent labels of Alexa 700-succinimide (red) and Alexa 800-maleimide (green) were used to label total protein and reduced NOTCH3-Fc, respectively. Repeated 3 times to confirm results.

b. Graphical representation of relative amount of reduced NOTCH3-Fc to total NOTCH3-Fc present in samples. Quantification done by taking ratio of Alexa 800-Maleimide (AM) fluorescence to Alexa 700-succinimide (AS) fluorescence normalized to background fluorescence. Data expressed as ratio to Lane 1 data (ie. "2" is equivalent to double the normalized AM/AS ratio calculated for Lane 1).

Towards a Mechanism of CADASIL

CADASIL has been linked to mutations to the NOTCH3 gene, which controls the production of the NOTCH3 protein. NOTCH3 is a transmembrane protein with an extracellular segment composed of 34 EGF-like domains, each of which contains 3 pairs of conserved cys-

teine residues that form disulfide bonds with each other. The majority of CADASIL-linked mutations to NOTCH3 result in an odd number of cysteine residues on this domain. This odd number disrupts disulfide bonding and leads to an overall reduction of the protein. Ongoing research in the Wang lab has found that the N-terminal fragment of NOTCH3 (NTF) is cleaved from reduced NOTCH3 and then goes on to reduce more disulfide bonds to form multiply-reduced cysteine NOTCH3. Certain subtypes of the conserved EGF-like domain on the NOTCH3 protein were shown to contain an active calcium-binding site. It is possible that the binding of calcium to these EGF-like domains results in conformational changes within NOTCH3 which alters the rate of its redox reaction with NTF. Indeed, our results demonstrate that the sequestration of Ca^{2+} ions by EGTA increases the reduction of NOTCH3 in the presence of NTF, while supplementation with Ca^{2+} ions via $CaCl_2$ decreases this NTF-induced NOTCH3 reduction. This suggests that Ca^{2+} ions play a role in slowing or inhibiting the reaction between NOTCH3 and NTF.

Thus, we hypothesize that calcium may influence the development of pathological NOTCH3 in CADA-SIL patients. Consistent with this hypothesis, reduced forms of the NOTCH3 protein are enriched in the brains of CADASIL patients. In the future, ensuring that the cerebrovascular environment is saturated with Ca^{2+} ions may be a method for preventing deleterious reduction of NOTCH3. Nevertheless, a concern for such treatment is hypercalcemia as physiological concentrations of Ca^{2+} is disturbed. If the amount of calcium needed for therapy is unsafe for patients, the development of synthetic ligands may circumvent this limitation. Further research into the structural changes that take place when calcium binds NOTCH3 could lend insight into how such ligands might be designed.

We have not directly investigated whether the calcium-dependent decrease in NOTCH3 reduction is

"By using safe methods for raising target calcium levels, or by developing other ways to manipulate the rate of reduction of NOTCH3, we may be able to slow the progression of CADASIL by slowing the production of the abnormal form of NOTCH3."

```
PPCLDGSPCA NGGRCTQLPS REAACLCPPG WVGERCQLED PCHSGPCAGR GVCQSSVVAG TARFSCRCPR GFRGPDCSLP DPCLSSPCAH GARCSVGPDG
RFLCSCPPGY QGRSCRSDVD ECRVGEPCRH GGTCLNTPGS FRCQCPAGYT GPLCENPAVP CAPSPCRNGG TCRQSGDLTY DCACLPGFEG QNCEVNVDDC
PGHRCLNGGT CVDGVNTYNC QCPPEWTGQF CTEDVDECQL QPNACHNGGT CFNTLGGHSC VCVNGWTGES CSQNIDDCAT AVCFHGATCH DRVASFYCAC
PMGKTGLLCH LDDACVSNPC HEDAICDTNP VNGRAICTCP PGFTGGACDQ DVDECSIGAN PCEHLGRCVN TQGSFLCQCG RGYTGPRCET DVNECLSGPC
RNQATCLDRI GQFTCICMAG FTGTYCEVDI DECQSSPCVN GGVCKDRVNG FSCTCPSGFS GSTCQLDVDE CASTPCRNGA KCVDQPDGYE CRCAEGFEGT
LCDRNVDDCS PDPCHHGRCV DGIASFSCAC APGYTGTRCE SQVDECRSQP CRHGGKCLDL VDKYLCRCPS GTTGVNCEVN IDDCASNPCT FGVCRDGINR
YDCVCQPGFT GPLCNVEINE CASSPCGEGG SCVDGENGFR CLCPPGSLPP LCLPPSHPCA HEPCSHGICY DAPGGFRCVC EPGWSGPRCS QSLARDACES
QPCRAGGTCS SDGMGFHCTC PPGVQGRQCE LLSPCTPNPC EHGGRCESAP GQLPVCSCPQ GWQGPRCQQD VDECAGPAPC GPHGICTNLA GSFSCTCHGG
YTGPSCDQDI NDCDPNPCLN GGSCQDGVGS FSCSCLPGFA GPRCARDVDE CLSNPCGPGT CTDHVASFTC TCPPGYGGFH CEQDLPDCSP SSCFNGGTCV
DGVNSFSCLC RPGYTGAHCQ HEADPCLSRP CLHGGVCSAA HPGFRCTCLE SFTGPQCQTL VDWCSRQPCQ NGGRCVQTGA YCLCPPGWSG RLCDIRSLPC
REAAAQIGVR LEQLCQAGGQ CVDEDSSHYC VCPEGRTGSH CEQEVDPCLA QPCQHGGTCR GYMGGYMCEC LPGYNGDNCE DDVDECASQP CQHGGSCIDL
VARYLCSCPP GTLGVLCEIN EDDCGPGPPL DSGPRCLHNG TCVDLVGGFR CTCPPGYTGL RCEADINECR SGACHAAHTR DCLQDPGGGF RCLCHAGFSG
PRCQTVLSPC ESQPCQHGGQ CRPSPGPGGG LTFTCHCAQP FWGPRCERVA RSCRELQCPV GVPCQQTPRG PRCACPPGLS GPSCRSFPGS PPGASNASCA
AAPCLHGGSC RPAPLAPFFR CACAQGWTGP RCEAPAAAPE VSEEPRCPRA ACQAKRGDQR CDRECNSPGC GWDGGDCSLS VGDPWRQCEA LQCWRLFNNS
RCDPACSSPA CLYDNFDCHA GGRERTCNPV YEKYCADHFA DGRCDQGCNT EECGWDGLDC ASEVPALLAR
```

Figure 3 - Expected Calcium-Binding EGF-Like Domains on NOTCH3
Amino Acid sequence of NOTCH3 protein [only portion of NOTCH3 containing EGF-like domains shown). Segments expected to correspond to calcium-binding EGF-like domains highlighted in green. Segment corresponding to EGF-like domain present on NTF is underlined. (Note: boundaries between adjacent EGF-like domains not marked)

due to structural changes in NTF or NOTCH3, both of which could be responsible for observed effect. Two plausible mechanisms could be involved: (1) calcium binds EGF-like domains on NOTCH3, stabilizes the disulfide bonds on these domains and prevents their reduction, (2) calcium binds the EGF-like domain on NTF, stabilizes the disulfide bond and prevents the formation of free thiols which reduce disulfide bonds on NOTCH3. However, our analysis of the NOTCH3 amino acid sequence suggests that NOTCH3's first EGF-like domain is not calcium-binding (Figure 3), while numerous downstream EGF-like domains have a higher calcium affinity than the first domain. Thus, it is more likely that calcium binds to NOTCH3 and stabilizes NOTCH3 against the reductive effects of NTF. In future studies, we could express NOTCH3 fragments that lack calcium-binding EGF repeats to confirm that these constructs do not demonstrate EGTA or calcium sensitivity.

Future studies may also further explore the effects of calcium on CADASIL in vivo. For this purpose, the Wang lab has developed a novel NTF-expressing mouse model which is being monitored for CADASIL symptoms. Should such symptoms be present, controlled supplementation of calcium may be administered to see if disease progression can be slowed or halted as our results predict. A post-supplementation examination of the cerebral vasculature of these mice might also provide further insights into the macroscopic effects of Ca2+ ions.
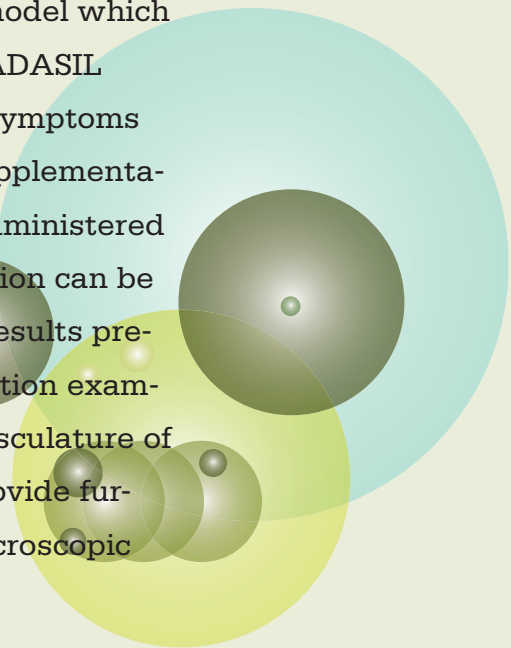
Implications for Treatment

Methods:

We have identified calcium as a potential factor which may slow the reduction of the NOTCH3 protein by NTF. This reduction produces a form of NOTCH3 which is structurally different from the functional protein and has been found to accumulate in the brains of CADASIL patients. Additionally, we have gathered evidence for a mechanism which explains the effect of calcium on the NOTCH3 protein. Treatment of CADASIL relies heavily on the slowing or reversal of the effects of mutant NOTCH3 protein. By using safe methods for raising target calcium levels, or by developing other ways to manipulate the rate of reduction of NOTCH3, we may be able to slow the progression of CADASIL by slowing the production of the abnormal form of NOTCH3. Thus, our study introduces calcium as a potential target for novel therapeutic treatments of CADASIL.

Fluorescent Labeling and Immunoprecipitation:

We used fluorescent tags and Fc-tagged NOTCH3 (NOTCH3-Fc) protein to observe NOTCH3 reduction. Purified NOTCH3-Fc protein with low free thiol content was collected from media of our NOTCH3-Fc-expressing cell line. Protein samples were incubated with solution of AS and AM (10 µL, 40 ng/mL AS, 20 ng/mL AM) for 30 minutes. The fluorescent labeling reagents Alexa 700-succinimide (AS) and Alexa 800-maleimide (AM) were used to label amine groups and free thiols, respectively. Samples were then incubated with Protein A-agarose overnight to pull down NOTCH3-Fc. PAGE was used to measure the amount of reduced NOTCH3 (visualized as AM fluorescence) in comparison to total amount of NOTCH3 (visualized as AS fluorescence) in each sample.

To investigate the effect of EGTA, we added 10mM EGTA to a mixture of NTF (1 µL, 1 µg/µL) and NOTCH3-Fc (4 µL, 1 µg/µL) solutions. For the analogous experiment with $CaCl_2$, we mixed the same mixture of NTF and NOTCH3-Fc with either 1.8 mM, 3.6 mM, 7.2 mM or 14.4 mM of $CaCl_2$.

References:

1. O'sullivan, M. (2010, 09). Imaging Small Vessel Disease: Lesion Topography, Networks, and Cognitive Deficits Investigated With MRI. Stroke, 41(10, Supplement 1). doi:10.1161/strokeaha.110.595314

2. Zhang, X., Lee, S. J., Young, M. F., & Wang, M. M. (2015, 01). The Small Leucine-Rich Proteoglycan BGN Accumulates in CADASIL and Binds to NOTCH3. Transl. Stroke Res. Translational Stroke Research, 6(2), 148-155. doi:10.1007/s12975-014-0379-1

3. Chabriat, H., Joutel, A., Dichgans, M., Tournier-Lasserve, E., & Bousser, M. (2009, 07). Cadasil. The Lancet Neurology, 8(7), 643-653. doi:10.1016/s1474-4422(09)70127-9

4. Joutel, A., Corpechot, C., Ducros, A., Vahedi, K., Chabriat, H., Mouton, P., . . . Tournier-Lasserve, E. (1996, 10). Notch3 mutations in CADASIL, a hereditary adult-onset condition causing stroke and dementia. Nature, 383(6602), 707-710. doi:10.1038/383707a0

5. Dong, H., Blaivas, M., & Wang, M. M. (2012, 05). Bidirectional encroachment of collagen into the tunica media in cerebral autosomal dominant arteriopathy with subcortical infarcts and leukoencephalopathy. Brain Research, 1456, 64-71. doi:10.1016/j.brainres.2012.03.037

6. Donahue, C. P., & Kosik, K. S. (2004, 01). Distribution pattern of Notch3 mutations suggests a gain-of-function mechanism for CADASIL. Genomics, 83(1), 59-65. doi:10.1016/s0888- 7543(03)00206-4

7. Zhang, X., Lee, S. J., Young, K. Z., Josephson, D. A., Geschwind, M. D., & Wang, M. M. (2014, 10). Latent NOTCH3 epitopes unmasked in CADASIL and regulated by protein redox state. Brain Research, 1583, 230-236. doi:10.1016/j.brainres.2014.08.018

8. Joutel, A., Vahedi, K., Corpechot, C., Troesch, A., Chabriat, H., Vayssière, C., . . . Tournier- Lasserve, E. (1997, 11). Strong clustering and stereotyped nature of Notch3 mutations in CADASIL patients. The Lancet, 350(9090), 1511- 1515. doi:10.1016/s0140-6736(97)08083-5

9. Selander-Sunnerhagen, M., Ullner, M., Persson, M., Teleman, O., Stenflo, J., & Drakenberg, T. (1994, 05). How An Epidermal Growth Factor (Egf)-Like Domain Binds Calcium-High Resolution Nmr Structure Of The Calcium Form Of The Nh2-Terminal Egf-Like Domain In Coagulation Factor X. doi:10.2210/pdb1ccf/pdb

10. EMBL-EBI, I. (n.d.). InterPro. Retrieved September 23, 2016, from http://www.ebi.ac.uk/interpro/entry/IPR018097

Simulation & Optimization of Surface Losses in Superconducting Qubits

Aaron Young

Mentor: Professor Oskar Painter

October 30, 2016

Abstract

A significant challenge in implementing scalable quantum computing systems is isolating qubits from their environment. By reducing the channels into which the qubit can decay, qubit coherence time, and thus the number of useful sequential logical operations that can be done on an entangled set of qubits, increases. Coherence times in state of the art superconducting (SC) qubits are primarily limited by coupling between the qubits and two level system (TLS) defects in the thin amorphous oxide layers that form on and between the metal and substrate that make up these devices. In order to minimize this coupling, we develop a series of nite element method (FEM) simulations that accurately model the electric field distributions in these devices under operating conditions. This allows us to probe the properties of any extraneous modes that are excited in the system, as well as the participation ratios of the various materials and interfaces present in the device. Using the results of these simulations we hope to optimize our designs to divert electric fields from regions of high loss, increasing resonator Q and qubit coherence time.

I. Introduction

Historically, the greatest challenge in implementing quantum computing has been isolating the fragile state of a quantum device from its environment to avoid decoherence [1]. The two loss mechanisms that limit the coherence times of state of the art superconducting qubits are surface losses associated with the thin amorphous oxide layers that grow on and between the metal and substrate that make up the qubits [2], and coupling of the superconducting circuitry to extraneous modes [1]. Recent advances have yielded improved superconducting qubit designs like the transmon that can reach the coherence times required to begin tackling the problem of decoherence from the perspective of error correction, rather than error prevention [3]. Simple error correction schemes that protect against bit flip errors like the 1D surface code have successfully been demonstrated [4]. However, to realize truly improved coherence times through error correction, we need to implement error correcting codes that protect against both bit and phase flip errors. Many such codes exist, including particularly promising examples like the full 2D surface code, and color gauge code [5]. To realize these codes, we must be able to scale up to systems of many qubits. As such, the challenge facing quantum computing is no longer simply a matter of isolation and shielding, and instead involves the conflicting requirements of design-ing systems of qubits that are both suciently isolated from the environment, and strongly coupled together.

Currently, the best coherence times in supercon-ducting qubits are achieved in 3D cavity transmons, reaching hundreds of microseconds [6], however, such designs become unwieldy when coupled together. 3D transmons are successful because they delocalize the electric field in the device, spreading it through a large conductive cavity and away from lossy defects on the surface of the chip. However, it is exceedingly difficult to couple more than two of these large cavities together, making the complicated connections required in more advanced error correction schemes like the color gauge code completely unfeasible. Instead, many groups are turning to planar transmon geometries, replacing large conductive cavities with a small transmission line resonator [3]. Many such devices can be patterned on a single chip through conventional lithographic techniques borrowed from the electronics industry, vastly simplifying fabrication. The downside is that compact resonator geometries focus the electric field near lossy surface defects, dramatically reducing coherence time. To address this problem, we develop a series of finite element method (FEM) simulation tools to simulate the electric field distributions in our devices under operating conditions. This both helps us classify the strength of coupling to extraneous modes, and the participation ratios of different materials present in the device. Such simulations will allow us to optimize our designs to minimize the effect of these dynamics, yielding devices with improved coherence times.

The challenge facing quantum computing is no longer simply a matter of isolation and shielding, and instead involves the conflicting requirements of designing systems of qubits that are both sufficiently isolated from the environment, and strongly coupled together.
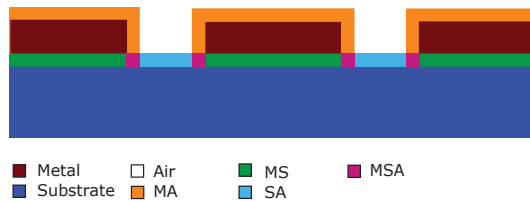
Figure 1: Cartoon cross section of a CPW, illustrating the various regions and interfaces studied.

II. Methods

The goal of the following set of simulations is twofold: first, the simulations resonantly excite various geometries in an attempt to analyze the various stable modes in the system, and the relative coupling strengths to each mode. Second, the participation ratios of each region in the simulation are extracted, including the three bulk regions classified by air (or vacuum), substrate, metal, and the various oxide interfaces between these regions, classified by metal-air (MA), metal-substrate (MS), substrate-air (SA), and metal-substrate-air (MSA)* Figure 1. These participation ratios are evaluated by taking the ratio between the electric field energy in a given region, and the total electric field energy in the system:

$$p_i = \frac{\epsilon_i}{W} \int_{v_i} |E|^2 dv, \qquad (1)$$

where p_i is the participation ratio of region v_i, which has permittivity E_i, E is the electric field, and W is the total electric field energy. If the loss tangent of each material is known, the quality factor, Q, can be directly retrieved from these calculations:

$$Q = \frac{1}{\sum_i p_i \tan \delta_i}, \qquad (2)$$

where $tan(i)$ is the loss tangent of a given region. The primary diffculty in simulating superconducting qubit geometries is the vast disparity in length scales present within each device, ranging from oxide layers that are a few nanometers thick, to

Figure 2: Schematic of the symmetric CPW mode (top), and antisymmetric slotline mode (bottom). The intensity plot and vectors illustrate the magnitude and intensity of the displacement field respectively. While the scale for the intensity plot is arbitrary, notice that the vast majority of the displacement field, and therefore the electric field energy, is contained in the substrate due to its higher dielectric constant.

packaging and resonator structures, which are on the scale of millimeters. In the case of FEM simulations, these geometries would either involve meshes far too dense to solve for in a reasonable amount of time, or extremely high aspect ratio mesh elements that would yield unphysical results. As such, our simulations are broken into 3 generations of increasing abstraction, with the results of each generation providing the basis for simplifying assumptions made in the next generation. All simulations were carried out in either the Electromagnetic Waves or Electrostatics module in COMSOL Multiphysics.

Due to the signicantly reduced computational complexity of 2D FEM simulations compared to 3D FEM, cross-sectional simulations serve as a natural starting point for analysis. The first generation of simulations involved 2D eigenmode analysis on idealized cross sections of the coplanar waveguide (CPW) geometries used in our devices. These simulations provided accurate depictions of the stable modes of propagation in idealized devices, namely the symmetric (CPW) and antisymmetric (slotline) modes* (Figure 2). These eigenmode problems are

*While the MSA region, where all three bulk regions meet, is comparatively minuscule by volume, these sharp boundaries are where singularities in the electric field tend to form, and so the participation ratio of the MSA region is on roughly equal footing with the other three interfaces.
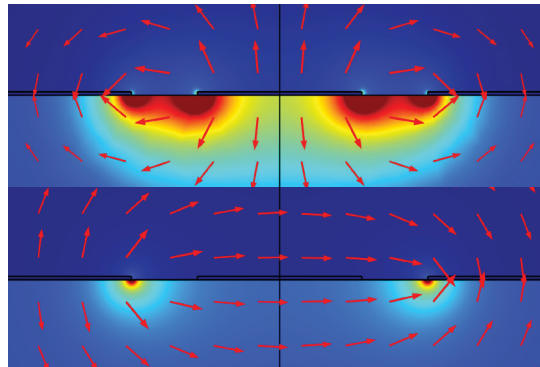
* With the CPW mode being the desired mode we use for signal transfer, and the slotline mode being the most strongly coupled to of the unwanted higher order modes of the system.

very difficult to get a meaningful solution for on all but the simplest geometries. In order to eventually solve for field distributions on more complex geometries, we replicated the stable modes by applying the appropriate boundary conditions to a quasi-static field simulation. Applying the appropriate potentials to the trace and ground planes, and terminating the simulation region with perfect magnetic conductor boundary conditions resulted in fields that agreed with the eigenmode solutions to within 0.1% in magnitude and direction at every point.

This quasi-static propagation model was the basis for the second generation of simulations, which leveraged the ease at which the quasistatic model could be solved on 2D meshes to simulate extremely high aspect ratio geometries†. In order for these simulations to accurately model the metal thickness and cross sectional profile of the CPW traces, as well as the thin lossy interfaces on and between the metal and substrate, adaptive meshing had to be introduced in order to properly resolve the singularities that occur at sharp edges in the geometry (Figure 3). It is important to note that since the participation ratios we are interested in involve integrating over these singularities, as long as the mesh is sufficiently fine near the singularity the solution converges. Away from sharp features, the electric field is effectively constant throughout the oxide layer. As such, we developed a series of simpler models that evaluated the participation ratio of the oxide layers by doing a contour integral involving a scale factor to account for oxide thickness, rather than directly accounting for the oxide in the geometry:

$$ p_i = \frac{\epsilon_i t_i}{\lambda} \int_{c_i} |E|^2 dl, \qquad (3) $$

---

† Typical geometries had CPW features on the scale of millimeters, with oxide layers 2-3nm thick.

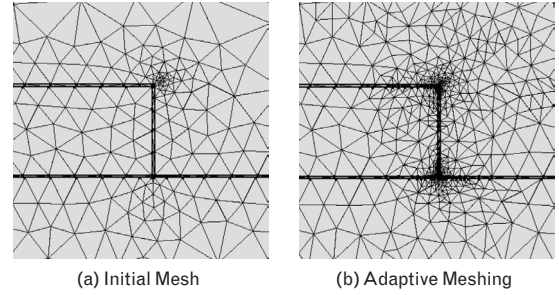(a) Initial Mesh   (b) Adaptive Meshing

Figure 3: Example of adaptive meshing near the edge of a trace. The initial mesh (a) is established and solved. Additional nodes are added to the mesh where previous solution varied rapidly (b), and the new mesh is solved. This process continues iteratively until the solution satisfies user-defined convergence conditions. Higher order adaptive meshes are omitted for visual clarity.

where ci is the contour of interest, ti is the real thickness of the interface along the contour, and λ is the electric field energy per unit length of waveguide. A separate point evaluation accounted for the contribution to participation from corners and sharp features:

$$ p_i = \frac{\alpha \epsilon_i t_i^2}{\lambda} |E(\vec{r_i})|^2, \qquad (4) $$

where $\vec{r_i}$ is the point of interest, and α is a shape factor ranging from 0 for a completely skew quadrilateral, to 1 for a square. This greatly reduced mesh density, while preserving the accuracy of participation ratio calculations, with participation ratios differing by less than 5% in all regions, and in all tested geometries.

Removing the high aspect ratio oxide layers from the geometry allowed for a third generation of full 3D simulations. In this case, the contour integrals

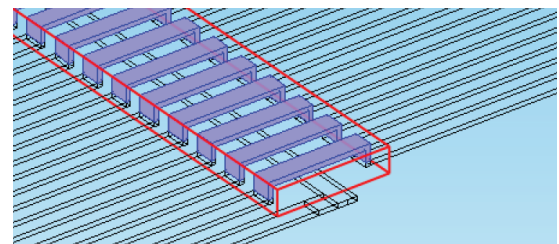**Figure 4:** Example of automatic boundary classification. In this case the model recognizes a series of bridge features, and partitions them from the rest of the geometry (red box). The partitioned features are classified by material, and the relevant interfaces are defined. The simulation parses the entire geometry in this manner, automatically assigning the relevant integrals and evaluations to calculate participation ratios.

and point evaluations used to evaluate surface participation ratios are replaced by surface and contour integrals respectively, in addition to a set of point evaluations at vertices in the geometry. Due to the tedium involved in defining the many interfaces and boundaries in complex 3D geometries, these simulations are designed to be highly adaptive, and automatically define the various domains and integrations to be evaluated based on material properties* (Figure 4). These full 3D simulations serve as a very effective tool to quickly evaluate the participation ratios and resonant behavior of arbitrary planar geometries on chip.

III. Results

A series of studies were conducted with the second generation simulations in an attempt to reduce the participation ratios in lossy regions of the device. The most straightforward study involved varying trace widths, while maintaining impedance matching. As expected, increasing trace width delocalizes the field, reducing the participation of the MA, MS, SA, and MSA interfaces, while increasing the participation of the substrate (Figure 5). The result is a quality factor that asymptotes to the value set by the loss tangent of the substrate, which is assumed to be 5 10 6 for Si at cryogenic temperatures [7] (yielding an ideal Q of $1=\tan(Si) = 2 \cdot 10^5$)† (Figure 6). For our current devices, with a center trace width of 5m and a corresponding air gap of 3m to achieve an impedance of 50, the participation ratio of the substrate and air were 91.67% and 8.17% respectively, yielding a Q of 1:27 105 assuming that all oxide interfaces had a loss tangent of 0:002 [7].

---

* e.g. the boundary between a conductive domain and an air box is automatically classied as a metal-air interface, and has the appropriate evaluations assigned to it.

† This approximation turns out to be too high. Comparison with the observed Qs of our devices suggests a loss tangent of roughly 1·10-6, which is in agreement with [8]. Due to the lack of consensus on the loss tangent of Si at cryogenic temperatures, it is more instructive to consider participation ratios or relative Q, rather than the actual value of Q.
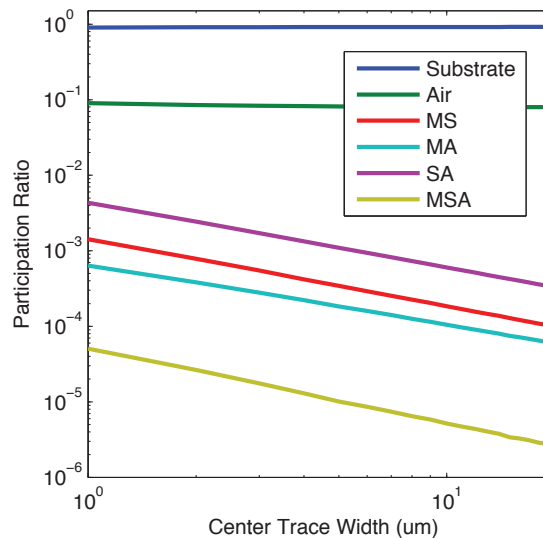

Figure 5: Participation ratios of the various regions of a CPW, as a function of center trace width, assuming that the lossy interfaces have a dielectric constant of 10 [7]. The outer trace width is established by analytically solving for a dimension that yields an impedance of 50. Notice that MS and MA participations are separated by roughly an order of magnitude, consistent with the ratio between the dielectric constant of silicon and air (≈11:7). As expected, the participation ratios of the lossy interfaces drop to roughly like 1=r where r is the CPW size, proportional to center trace width.
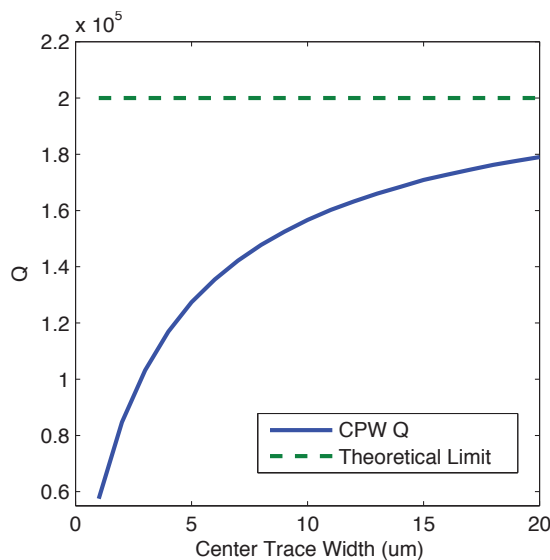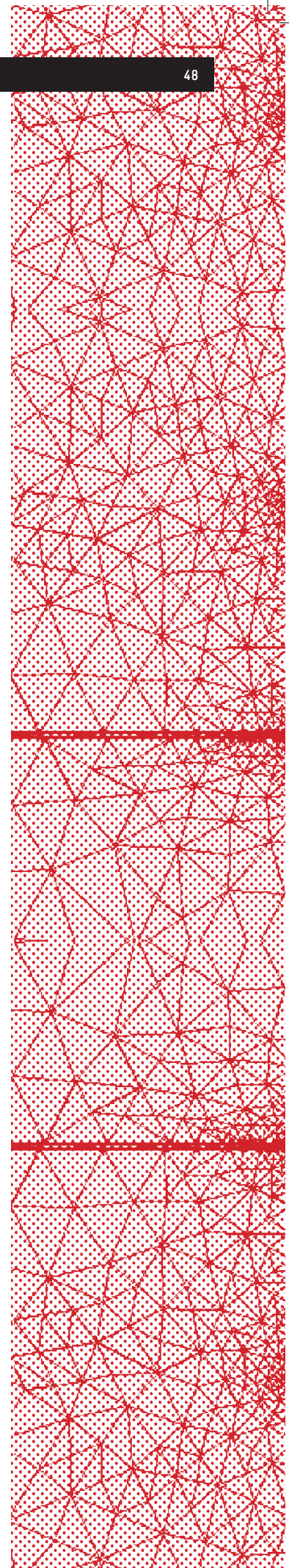

Figure 6: CPW quality as a function of center trace width, assuming a loss tangent of 5·10-6 in silicon, and 0:002 in the lossy oxide interfaces. As the geometry size increases, the quality asymptotes to the value associated with electromagnetic wave propagation through bulk silicon.
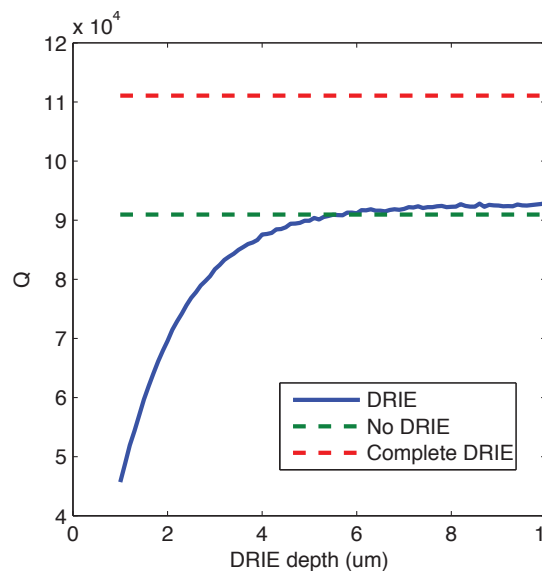
Figure 7: CPW quality as a function of DRIE depth, assuming the same material properties as above, with 5m center trace and 3m gap. A shallow DRIE effectively introduces a pair of MA and SA interfaces in place of the MS interface, drastically reducing Q. An etch deeper than 5m pulls the SA interface sufficiently far from the region of high electric field to result in a net gain in CPW quality, however, the gains are well below 0.2% for up to a 10m etch, and under 25% in the ideal case of an infinitely deep etch.

The participation ratios calculated by these simulations were within 3% of the values previously reported by the Martinis group [7] for all geometries tested. We find that of the lossy interfaces, the SA and MS regions dominate. Subsequent simulations targeted these two interfaces, attempting to direct the electric field away from them. One scheme to target these interfaces that has been attempted experimentally is a deep reactive ion etch (DRIE) that attacks the substrate from under the conductor, removing the MS interface entirely [9]. We find, however, that because the dielectric constant of air is low compared to that of the oxide layers, removing the substrate increases the overall participation ratio of the oxide layers. As such, even in the limiting case where the substrate is completely removed, and the device is suspended in a lossless vacuum, the increase in Q is essentially negligible (Figure 7). This explains the relative lack of success groups have had with the DRIE process* [9].

---

* Furthermore, the very aggressive DRIE process is also likely to reduce the surface quality of the device, increasing the loss tangent associated with the SA and MA interfaces.

Another process that has been considered is an undercut that targets the exposed SA regions of the device, cutting out a trench surrounding the conductive traces. This removes the MSA region, and moves the SA interface further from the singularities in the field, while still containing most of the electric field to within the substrate. Surprisingly, while an infinitely deep undercut reduces Q by about 10%, a small undercut of around 2nm results in higher simulated Q than no undercut (Figure 8). This unintuitive behavior is due to the fact that the field is strongest directly between the edge of the trace and ground plane. A small undercut shifts the SA interface out of this region, increasing Q, however, removing too much of the substrate confines the field strongly to the region of the substrate directly below the signal carrying trace, and increases the participation ratio of the MA interface due to the comparatively low dielectric constant of air. It is important to note, however, that undercuts below 1nm are not being properly resolved by the mesh, introducing additional singularities in the electric field at the bottom of the undercut†.

In an attempt to direct the electric field with a less aggressive fabrication step that is less likely to reduce the surface quality of the device, we considered an undercut that targeted the metal layer, changing the angle of the side-walls of the CPW. This increases the curvature of the trace boundary in air and reduces the curvature near the substrate, forcing more of the electric field into the air (which is lossless) and away from the bulk substrate, MS, and MA interfaces. Larger deviations from vertical results in a longer CPW edge, and thus MA interface, resulting in roughly symmetric scaling of MA participation about 0 (Figure 9). Reasonable undercuts were found to increase Qs by about 20% (Figure 10).

---

† This is why very short undercuts do not result in Qs representative of the same geometry with no undercut. Until the undercut depth is actually zero, the additional singularities increase the participation of the lossy interfaces. Due to this unphysical behavior, the simulations should not be trusted for very short undercuts.

It is critical to identify useful processing techniques and desirable device features through simulation before attempting time-consuming and expensive fabrication studies.

The first application of the full 3D model has involved simulation of a spiral inductor used in MEMS devices fabricated in the lab. In an attempt to increase the quality of the resonators made with these inductors, the entire device sits on top of a thin free-standing silicon membrane formed on a silicon on insulator (SOI) wafer [10]. Because the insulating layer of amorphous silicon dioxide is very lossy, any fields contained within it are rapidly dissipated, reducing Q. To avoid this it is important to quantify how the participation ratio of this region varies with how far the boundaries of the undercut region, where the silicon dioxide is removed, are from the device. Preliminary studies show that at resonance, the field is very tightly confined to the inductor, and so the participation ratio of the amorphous region is effectively constant: the participation ratio at resonance given a separation between device and amorphous region ranging between 15m and 115m ranges only between 11:4 10 5 and 8 10 5. Off resonance, the field is signicantly less localized, and so the participation ratio rises dramatically, reaching values as high as 10 1 when detuned from resonance by 150MHz (Figure 11).

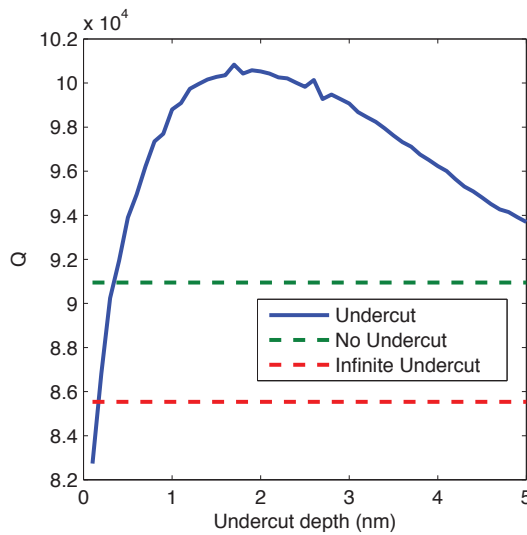**Figure 8:** CPW quality as a function of undercut depth, assuming the same material properties and CPW dimensions as above. Undercutting the CPW by 2nm can increase the Q by as much as 15%, with deeper undercuts asymptotically approaching a limiting value of Q 10% less than an unaltered CPW.
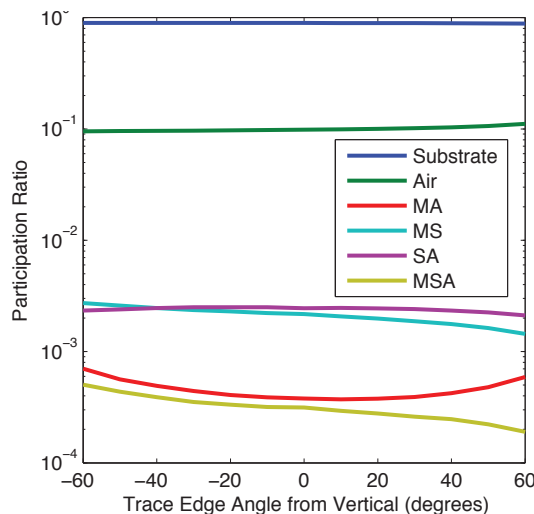

Figure 9: Participation ratios as a function of CPW edge angle, assuming the same material properties and CPW dimensions as above.
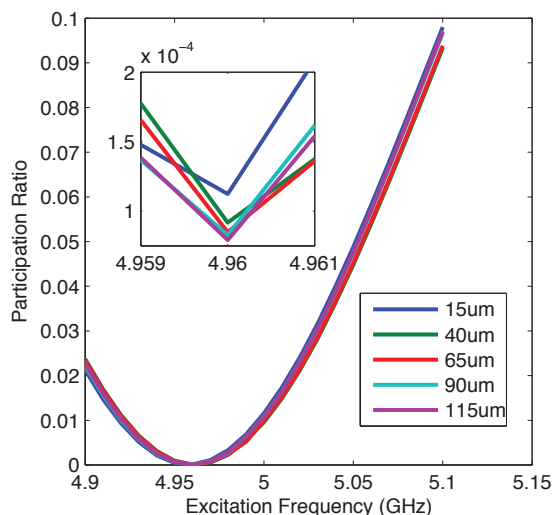
Figure 11: Participation ratio of the amorphous SiO_2 region of the device at varying excitation frequencies. Notice that all geometries follow the same trend of reduced participation due to strong localization of the field at resonance. Inset: Participation ratio's near resonance at 4.96GHz. At resonance participation scales roughly as expected with increasing gap from the device geometry. Note: This data is not finalized. The line crossings observed are likely due to overly lax convergence criterion, and xoarse frequency sweep.
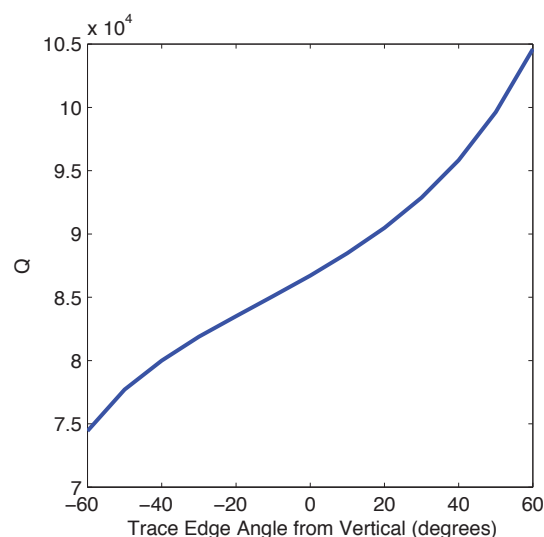

Figure 10: CPW quality as a function of edge angle, assuming the same material properties and dimensions as above. Note that the non-linear scaling is partially due to the angular parameterization. At ±90° the CPW has infinite curvature either in air or in substrate, resulting in very high or low Qs respectively.

IV. Discussion

In recent years, as the superconducting qubit community has moved towards fabrication on silicon substrates, a huge range of additional processing and fabrication techniques borrowed from the electronics industry have been made available [3]. While many groups have attempted to optimize device quality with these processing techniques, the abundance of untested materials and fabrication protocols make it difficult to do any sort of comprehensive study. As such it becomes critical to identify useful processing techniques and desirable device features through simulation before attempting time consuming and expensive fabrication studies. This study has attempted to address the diffculty of simulating surface losses in superconducting devices by making a series of simplifying assumptions that are veried by high fidelity 2D cross sectional simulations. The second generation simulations both provided insight into optimizing trace dimensions and profiling, and quantied the behavior of the electric fields in the thin lossy oxide layers surrounding the device. The third generation model provides a readily solvable* adaptive 3D simulation that serves as an effective prototyping and design tool, giving a reasonable estimate of participation ratios and device quality for arbitrary circuit geometries. As we scale towards the larger and more complex networks of quantum devices necessary for error correction, and eventually quantum computing and simulation, it becomes necessary to implement robust forms of routing, integration, device design, and on chip shielding that can help to prevent crosstalk and unwanted coupling, as well as component design that minimizes participation of lossy surfaces in the device. The models developed in this study will hopefully serve the group as a useful preliminary design tool to help achieve such optimization.

---

* In the past, similar 3D simulations of the spiral inductor studied took nearly an hour to solve for each position in a sweep, while the current model solves each position in under 5 minutes on the same hardware due to the simplifying assumptions described above, and careful use of adaptive meshing.

V. Acknowledgements

References

[1]   J. M. Martinis and A. Megrant, \UCSB final report for the CSQ program: Review of decoherence and materials physics for superconducting qubits," ArXiv e-prints, Oct. 2014.

[2]   C. Wang, C. Axline, Y. Y. Gao, T. Brecht, Y. Chu, L. Frunzio, M. H. Devoret, and R. J. Schoelkopf, Surface participation and dielectric loss in superconducting qubits," Applied Physics Letters, vol. 107, p. 162601, Oct. 2015.

[3]   R. Barends, J. Kelly, A. Megrant, D. Sank, E. Jerey, Y. Chen, Y. Yin, B. Chiaro, J. Mutus, C. Neill, P. O'Malley, P. Roushan, J. Wenner, T. C. White, A. N. Cleland, and J. M. Martinis, Coherent Josephson Qubit Suitable for Scalable Quantum Integrated Circuits," Physical Review Letters, vol. 111, p. 080502, Aug. 2013.

[4]   J. Kelly, R. Barends, A. G. Fowler, A. Megrant, E. Jerey, T. C. White, D. Sank, J. Y. Mutus, B. Campbell, Y. Chen, Z. Chen, B. Chiaro, A. Dunsworth, I.-C. Hoi, C. Neill, P. J. J. O'Malley, C. Quintana, P. Roushan, A. Vainsencher, J. Wenner, A. N. Cleland, and J. M. Martinis, State preservation by repetitive error detection in a superconducting quantum circuit," Nature, vol. 519, pp. 66{69, Mar. 2015.

[5]   A. Kubica and M. E. Beverland, Universal transversal gates with color codes: A simplified approach," Phys. Rev. A, vol. 91, p. 032330, Mar. 2015.

[6]   H. Paik, D. I. Schuster, L. S. Bishop, G. Kirchmair, G. Catelani, A. P. Sears, B. R. Johnson, M. J. Reagor, L. Frunzio, L. I. Glazman, S. M. Girvin, M. H. Devoret, and R. J. Schoelkopf, Observation of high coherence in josephson junction qubits measured in a three-dimensional circuit qed architecture," Phys. Rev. Lett., vol. 107, p. 240501, Dec 2011.

[7]   J. Wenner, R. Barends, R. C. Bialczak, Y. Chen, J. Kelly, E. Lucero, M. Mariantoni, A. Megrant, P. J. J. O'Malley, D. Sank, A. Vainsencher, H. Wang, T. C. White, Y. Yin, J. Zhao, A. N. Cleland, and J. M. Martinis, Surface loss simulations of superconducting coplanar wave-guide resonators," Applied Physics Letters, vol. 99, p. 113513, Sept. 2011.

[8]   H. S. Jung, W. I. Yang, M. S. Cho, K. N. Joo, and S. Y. Lee, Microwave losses of undoped n-type silicon and undoped 4h-sic-single crystals at cryogenic temperatures," Electronic Materials Letters, vol. 10, no. 3, pp. 541{549, 2014.

[9]   Y. Chu, C. Axline, C. Wang, T. Brecht, Y. Y. Gao, L. Frunzio, and R. J. Schoelkopf, Suspending superconducting qubits by silicon micromachining," Applied Physics Letters, vol. 109, no. 11, 2016.

[10] P. B. Dieterle, M. Kalaee, J. M. Fink, and O. Painter, \ Superconducting cavity electromechanics on a silicon-on-insulator platform," Phys. Rev. Applied, vol. 6, p. 014013, Jul 2016.

Modelling Prices for Transportation Firms to Reduce Costs of Transporting Disabled Children to School

Brian Deng

Mentors: Charles R. Plott, Hsing-Yang Lee, and Travis D. Maron

Abstract

Transporting severely disabled children to school is costly and time-consuming. Considering that children with varied disabilities sit in the same bus, transportation providers have a difficult job trying to provide the accommodations that each child needs. Our experiment uses experimental economics to allow computer software to match unique transportation requirements to various transportation providers with specialized equipment. Both transportation providers and the children's families bid for a small duration of time, then the bidding data is processed so that the difference between the sum of the highest bids from those transported and the sum of the lowest offers from the transport providers, or the surplus, is maximized. The computer software also matches rider needs with vehicles that accommodate those needs. Multiple experiments varied from using a single route and a single-passenger vehicle capacity to using more complex routes and variable capacities to observe the behavior of both parties bidding. As a result, the efficiency is between 80% to 100% of the maximum surplus theoretically calculated.

Modeling Transportation Bids

Linear programming software takes advantage of linear algebra to solve allocation problems. All over the world, transporting severely disabled children to their schools is extremely costly. This research develops a model to match transportation demand with supply, and this model is tested in the city of Geelong, Australia. This experimental plan is based on the ideas of Banks, Ledyard, and Porter (1989) to understand allocative efficiency of markets. A method to make this situation more efficient involves multiple transportation firms (suppliers) and the children's family members (demanders), all of whom will bid their prices during a period of time to shape and coordinate the final offers, which will allow each child to be transported to school. An introductory theoretical model was first addressed by Plott, Lee, and Maron (2014), but is expanded to include more complex parameters, such as routes. In this research, the transportation firms are operating in a competitive product market. The bids are calculated and matched using a software computing program, MATLAB, by using algorithms and linear operators that are defined in Computational Formula 1. Continuous bidding is optimized so that the surplus, or the difference between the sum of winning (highest) bids from those transported and the sum of winning (lowest) offers from the transport providers, is maximized. The software will help the firms take the most efficient routes to reduce costs. If successful, each child can be matched with a specific transportation provider who can get them to school.

The codes in MATLAB are able to solve this linear programming problem, given the parameters. The parameters and variables are in the form of constrained inequalities, which are reorganized to a matrix form. During all of the experiments, the efficiency is 80% to 100% of the theoretical maximum surplus, calculated from MATLAB.

Computational Bidding Process

The aim of this project is for MATLAB to calculate the problem in Computational Formula 1, with the given parameters and constrained inequalities.

Computational Formula 1

Mathematical Sets and Matrices:

$N = \{1, 2, \dots, n\}$: number of students

$Q = \{1, 2, \dots, q\}$: number of qualities

$M = \{1, 2, \dots, m\}$: number of routes

$R = \{1, 2, \dots, r\}$: number of vehicle owners

$J = \{1, 2, \dots, j\}$: number of vehicles

η: number of vehicles each owner is allowed to supply

$S, J \times 1$: capacity of vehicles

$C, J \times Q$: availability of services on vehicles

$O, J \times R$: ownership matrix

$L, M \times N$: children on routes

$d, M \times 1$: route distance

$P, J \times 1$: asks placed by vehicle owners for vehicles

$U, Q \times N$: bids submitted by students for services

$u, R \times N$: bids submitted by students for vehicle owners

  (**Note:** Bidders can pay more for some brands and create a competition for better qualities not in the system).

$G, J \times 1$: asks placed by vehicle owners for a mile, "gasoline charge", in dollars per mile

$B, J \times N: B_{jn} = \left(\sum_{q=1}^{Q} C_{jq} U_{qn}\right) + \sum_{r=1}^{R} O_{jr} u_{rn}$

(total bids for vehicles)

  (**Note:** You can see the bids on brands here).

$Z, J \times N: Z_{jn} = 0$ if bid on vehicle j placed by student n is not winning, $Z_{jn} = 1$ if bid on vehicle j placed by student n is winning

$w, J \times 1: w_j = 0$ if vehicle j is not used, $w_j = 1$ if vehicle j is used

$X, J \times N: X_{jn} = 0$ if student n is not placed on vehicle j,

$X_{jn} = 1$ if student n is placed on vehicle j

$V, J \times M: V_{jm} = 0$ if route m is not assigned to vehicle j,

$V_{jm} = 1$ if route m is assigned to vehicle j

Objective Function to Solve, with Constraints:

$\max_{Z,w,X,V} \left[\sum_{j=1}^{J} \sum_{n=1}^{N} B_{jn} \cdot Z_{jn} - \sum_{j=1}^{J} P_j \cdot w_j - \sum_{j=1}^{J} \sum_{m=1}^{M} G_j \cdot d_m \cdot V_{jm}\right]$ such that:

Constraints:

$\sum_{n=1}^{N} X_{jn} \leq S_j \cdot w_j; j = 1, \dots, J$

$\sum_{j=1}^{J} X_{jn} \leq 1; n = 1, \dots, N$

$\sum_{j=1}^{J} w_j \cdot O_{jr} \leq \eta; r = 1, \dots, R$

(**Note:** A vehicle owner can sell rides on more than one vehicle. The limits on this appear here. Each owner is restricted to have no more than vehicles in use.)

$\sum_{m=1}^{M} V_{jm} = w_j; j = 1, \dots, J$

$\sum_{m=1}^{M} V_{jm} \cdot L_{mn} \geq X_{jn}; j = 1, \dots, J; n = 1, \dots, N$

$Z_{jn} \leq X_{jn}; j = 1, \dots, J; n = 1, \dots, N$

$0 \leq Z_{jn} \leq 1; j = 1, \dots, J; n = 1, \dots, N$

$0 \leq w_j \leq 1; j = 1, \dots, J$

$0 \leq X_{jn} \leq 1; j = 1, \dots, J; n = 1, \dots, N$

$0 \leq V_{jm} \leq 1; j = 1, \dots, J; m = 1, \dots, M$

This research develops a model to match transportation demand with supply, and this model is tested in the city of Geelong, Australia.

The demanders first submit bids in the computer software for the ride from their place of residence to the specific school, as shown in Figure 3. Additional bids depend on the various services (e.g. asthma care, blindness care) chosen, provided by different suppliers, who are vehicle owners. The suppliers list the services available within each vehicle, and submit their asking price to operate various vehicles, as shown in Figure 4. Each vehicle owner can declare different asking prices for different configurations of a vehicle. Then, the system goes through continuous (iterative) bidding and optimizes the net social benefit by using Computational Formula 1 to determine: least cost suppliers of vehicles, optimal vehicle sizes, vehicle service configurations, assigning disabled students to vehicles providing affordable and desired services, assigning passengers to fit the vehicle's capacity limits, and assigning routes to vehicles. The final costs and revenue will be distributed to students and suppliers, respectively. The system will also compute and maximize the surplus (sum of winning bids from demanders minus the sum of winning offers from suppliers). The constraints include the vehicle assignment count, vehicles not used over capacity, and students being assigned only one vehicle.

#2				
		#3		
	#1			
			#4	
				#5
	School			

Figure 1: Example of a Gridded Map with Students' Locations (Lines Are Streets with Fixed Parameters): **Note:** The location "school" can also be defined as an intermediate stop where some vehicles drop off students for other vehicles to pick up.

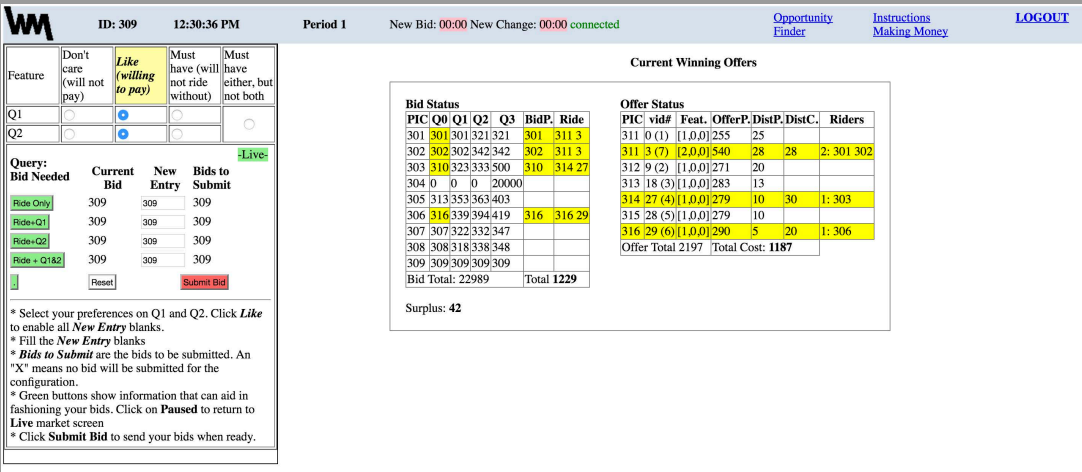| Routes (Matrix)								
Students	Route 1	Route 2	Route 3	Route 4	Route 5	Route 6	Route 7	Route 8
#1	0	1	0	0	0	0	1	1
#2	0	0	1	0	0	0	1	1
#3	0	0	0	1	0	0	0	1
#4	0	0	0	0	1	0	0	1
#5	0	0	0	0	1	0	0	0
School	1	1	1	1	1	1	1	1
Distance	d_1	d_2	d_3	d_4	d_5	d_6	d_7	d_8

Figure 2: Example Route Matrix.

Figure 3: Buyer Preferences.

Behaviors of both demanders and suppliers reached a high rate of efficiency (defined by at least 80%) after a duration of time.
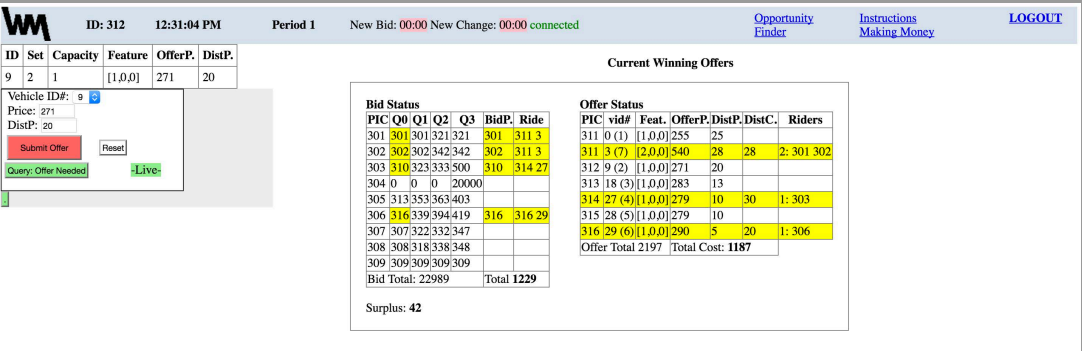

Figure 4: Seller Preferences.

Results

Using the experiment in July 14, 2016, there were 6 demanders and 6 suppliers. Each supplier had 3 vehicles, all of which have a capacity of 1 child. There were 2 different additional services, so each vehicle owner offered 3 options: ride only, ride with service #1, and ride with service #2. After the bidding period of 225 seconds, the experiment reached a surplus (also named 'value-costs') of 794.5 in Figure 5. Figure 6 shows the theoretical calculations from MATLAB (using Computational Formula 1), with a surplus of 794.5. Therefore, the efficiency is 100%.

Conclusions

The experiment of July 14, 2016, showed that the behaviors of both demanders and suppliers reached a high rate of efficiency (defined by at least 80%) after a duration of time. However, the limitations include having only 2 services for disabled children to use, and that each vehicle used has a limited capacity of 1 child. Generalizing this experiment to a broader range of vehicle capacities, various services, and various routes will eventually allow the school system in Geelong, Australia to take advantage of this linear programming software.
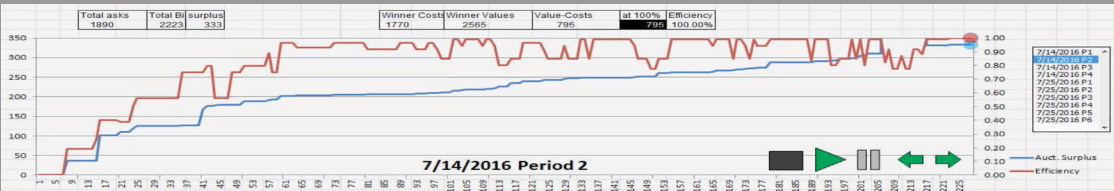
Figure 5: Seller Surplus and Efficiency of Experiment in July 14, 2016. The horizontal axis indicates time (in seconds). The left vertical axis indicates the auction's surplus (which steadily increases after 60 seconds). The right vertical axis indicates the efficiency (which fluctuates between 80% and 100% after 60 seconds).

			Win Veh.	Surplus							Winning Offers							Winning Bids
				794.5							1970							2764.5
PIC	VID#	$Cost		301	302	303	304	305	306		$Offer	301	302	303	304	305	306	$Bids
311	0(1)(1,0,0)	400	0	0	0	0	0	0	0	0	0	0	0	0	0	0	0	0
	1(1)(1,1,0)	425	1	0	0	0	1	0	0	1	425	0	0	0	635	0	0	635
	2(1)(1,0,1)	465	0	0	0	0	0	0	0	0	0	0	0	0	0	0	0	0
312	3(2)(1,0,0)	445	0	0	0	0	0	0	0	0	0	0	0	0	0	0	0	0
	4(2)(1,1,0)	470	1	0	0	1	0	0	0	1	470	0	0	672.5	0	0	0	672.5
	5(2)(1,0,1)	510	0	0	0	0	0	0	0	0	0	0	0	0	0	0	0	0
313	6(3)(1,0,0)	490	0	0	0	0	0	0	0	0	0	0	0	0	0	0	0	0
	7(3)(1,1,0)	515	1	0	1	0	0	0	0	1	515	0	710	0	0	0	0	710
	8(3)(1,0,1)	555	0	0	0	0	0	0	0	0	0	0	0	0	0	0	0	0
314	9(4)(1,0,0)	535	0	0	0	0	0	0	0	0	0	0	0	0	0	0	0	0
	10(4)(1,1,0)	560	1	1	0	0	0	0	0	1	560	747	0	0	0	0	0	747
	11(4)(1,0,1)	600	0	0	0	0	0	0	0	0	0	0	0	0	0	0	0	0
315	12(5)(1,0,0)	580	0	0	0	0	0	0	0	0	0	0	0	0	0	0	0	0
	13(5)(1,1,0)	605	0	0	0	0	0	0	0	0	0	0	0	0	0	0	0	0
	14(5)(1,0,1)	645	0	0	0	0	0	0	0	0	0	0	0	0	0	0	0	0
316	15(6)(1,0,0)	585	0	0	0	0	0	0	0	0	0	0	0	0	0	0	0	0
	16(6)(1,1,0)	600	0	0	0	0	0	0	0	0	0	0	0	0	0	0	0	0
	17(6)(1,0,1)	630	0	0	0	0	0	0	0	0	0	0	0	0	0	0	0	0
				1	1	1	1	0	0									

Figure 6: Matrix on left (orange background), where it shows if the bid of a student (#301 to #306) for a vehicle is winning. Matrix on right (orange background), where it shows the bidding prices of the winning students. This figure also shows the surplus as 794.5.

Further Reading

Banks, J. S., J. O. Ledyard, and D. P. Porter. 1989. "Allocating Uncertain and Unresponsive Resources: An Experimental Approach." RAND Journal of Economics 20 (1): 1–25.

Plott, Charles R., Hsing-Yang Lee, and Travis Maron. 2014. "The Continuous Combinatorial Auction Architecture." American Economic Review 104 (5): 452-56.

Acknowledgements